

---

## Task Title: TW2-TMSM-COOLIN: MOCK-UPS FOR THE TF AND CS TERMINAL REGIONS AND COOLING INLETS

---

### INTRODUCTION

---

Among our Association, the CEA-Cadarache Magnet Group is requested to assist the EFDA Close Support Unit Garching and the Superconducting Coils and Structures Division of the ITER International Team in the detailed design and manufacture of relevant mock-ups for some critical areas of the Toroidal Field (TF), Central Solenoid (CS) and Poloidal Field (PF) coil windings.

Mechanical testing at cryogenic temperatures of the mock-ups under relevant loads and number of cycles will be carried out at FZK Karlsruhe (TW3-TMSM-CRYTES) and ENEA Brasimone (TW1-TMS-SHKEYS). Euratom-CEA is requested to design the mock-ups in close collaboration with these two Groups and EFDA/ITER, coordinate the testing activity and report on the final test results. Our Association is responsible for the definition of the testing conditions (loads, number of cycles, temperature, etc.) under review and approval of EFDA/ITER.

The work includes three main activities:

- Design, manufacture and assistance to testing of mock-ups and samples of the Toroidal Field (TF) coil helium inlet;
- Design, manufacture and assistance to testing of mock-ups and samples of the Central Solenoid (CS) helium inlet;
- Design, manufacture and assistance to testing of mock-ups and samples of the bonded tails at the extremity of the windings of the Poloidal Field (PF) coils.

### 2006 ACTIVITIES

---

#### DEVELOPMENT OF THE CS COIL HELIUM INLET

##### Design and analysis

The CS conductor consists of a Nb<sub>3</sub>Sn cable-in-conduit with a central cooling channel, cooled by supercritical helium. The material used for the conductor jacket is stainless steel. The jacket inner diameter is 33.2 mm and the jacket outer square section is 49.9 mm×49.9 mm.

The CS modules are wound as hexa-pancakes (6 pancakes with a single conductor length) and quad-pancakes (4 pancakes with a single conductor length). Helium inlets are at the crossover regions on the inner bore between each double pancake and outlets are at the crossover regions and joints on the outside. The high field region is therefore cooled by the coldest helium. There are three helium inlets for each hexa-pancake and two for each quad-pancake. The inlets are located at the CS inner diameter, where cyclic tensile stresses are highest. In the CS jacket, the maximum

stress occurs at initial magnetization and reaches 470 MPa in the vertical sidewalls of the jacket. The helium inlet region requires, therefore, a local reinforcement to allow the opening in the conductor jacket without excessive stress intensification. The inlet must also provide a good distribution of helium in the six sub-cables of the conductor. A design of this inlet was suggested by IT to achieve these requirements. A model of the inlet was built and a F.E.M. analysis has led to a design optimisation. In addition, a manufacturing mock-up allowed to validate the feasibility of this kind of inlet which is characterised by a narrow groove of one cable twist pitch long. All this work was performed during year 2004.

##### Mock-ups manufacture

Unfortunately, due to development problems, no relevant material for the conductor jacket manufacture was available. It was then decided in agreement with EFDA and IT to cancel the mechanical qualification part of the contract. An hydraulic mock-up only was built in 2005 using a dummy TFMC cable which was jacketed with a square Valinox tube. A final length of 4 m of conductor was produced by ENEA. The helium inlet mock-up called CS-IN5 was manufactured in the middle of this conductor length and was tested in the beginning of year 2006.

##### Hydraulic qualification

The hydraulic qualification was performed on CS-IN5 in the OTHELLO test facility using GN2 at room temperature under relevant Reynolds conditions.

The ITER CS operating point is  $Q_c = 8$  g/s,  $P = 0.6$  MPa,  $T = 4.7$  K in supercritical Helium.

The conductor of the mock-up having not the same helium areas, the Reynolds analogy was made only in the annular area. The corresponding operating point with Nitrogen in our facility was determined to be  $Q_c = 60.0$  g/s,  $P = 0.1$  MPa,  $T = 300$  K.

The hydraulic path was symmetric as it is on the CS coils with temperature, pressure and flow rate sensors as shown in figure 1. Due to symmetry, the conductor flow rate was recorded at one side only. A specific preparation of each conductor end allow to separate each petal flow rate and to record it using a movable flow-meter. With this facility layout, pressure drop as well as flow repartition among the petals were recorded.

Four tests were performed: the first one with a 1.85 m conductor length at each inlet side, this length was then reduced to 1 m, 0.85 m and finally 0.41 m. With this process, the evolution of the flow rate distribution was checked at different distances from the inlet. The inlet pressure drop as well as the flow rate distribution were compared to reference pressure drop and flow rate distribution gained on a 4 m long TFMC conductor with a gas inlet at one end.

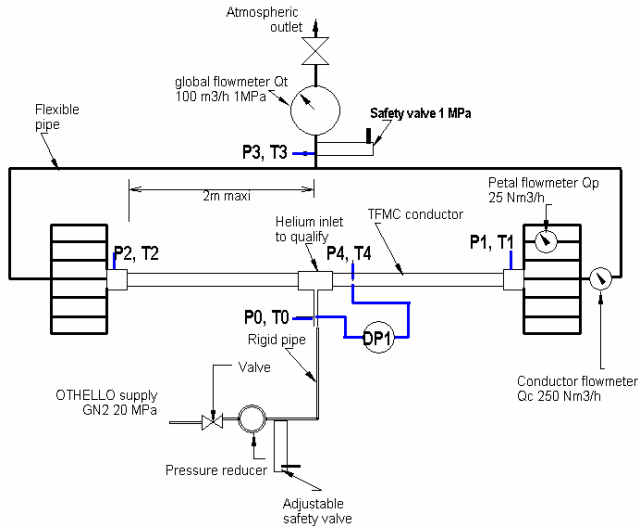


Figure 1: Hydraulic path of the OTHELLO test facility for inlet qualification

The pressure drop of the inlet was found to be quasi-linear with the conductor flow rate. It was interesting to compare the inlet pressure drop coefficient to the one of the unit length of conductor. However, in ITER type conductors, the hydraulics uses a dual channel with a high Reynolds inside central channel and a low Reynolds in the petals area. Then the conductor characterisation is not easy. For simplification, in the particular TFMF conductor geometry, a reduced pressure drop coefficient and a reduced Reynolds number independents of the wetted area  $A_c$  and hydraulic diameter  $D_h$  can be defined with respect to the global conductor mass flow rate  $Q_c$  and the measured pressure drop  $\Delta P$  as follows:

$$K^* = \frac{\rho \Delta P}{Q_c^2} \quad \text{Re}^* = \frac{Q_c}{\mu}$$

with  $K^* = \frac{K}{2A_c^2}$  and  $\text{Re}^* = \frac{\text{Re} A_c}{D_h}$

( $\rho$ ,  $\Delta P$ ,  $Q_c$ ,  $\mu$ ,  $A_c$ ,  $D_h$ ) in ( $\text{Kg/m}^3$ , MPa,  $\text{Kg/s}$ , Pa.s,  $\text{m}^2$ , m)

The reduced inlet pressure drop coefficient  $K^*$  was found to have a low dependency on the reduced Reynolds number  $\text{Re}^*$  in a same way that for the regular conductor unit length with a value lightly identical (figure 2).

The flow rate distribution among petals was recorded at 1.85 m, 1 m, 0.85 and 0.41 m from the inlet and compared to the one gained on our reference 4 m long straight conductor. The results at the CS operating point are summarised in table 1.

These results show some unexplained behaviour since the annular flow rate should be maximum near the inlet and should decrease when the distance to the inlet increases. Probably that the separation flow system was not perfect and has disturbed the results. Anyway, it can be concluded that with this helium inlet design, all the petals are well cooled by a flow rate higher than in a regular conductor.

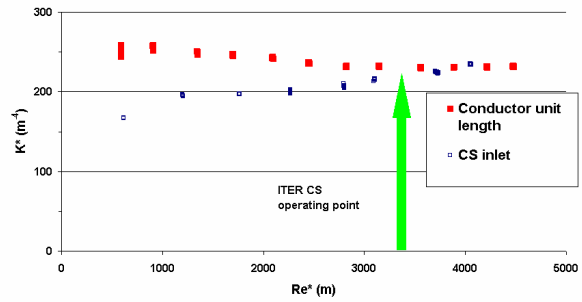


Figure 2: Reduced pressure drop coefficient of the CS inlet compared to the regular conductor unit length

Table 1: Flow rate ratios for the different studied configurations

	Petal 1	Petal 2	Petal 3	Petal 4	Petal 5	Petal 6	Annular
At 4 m of direct inlet	5.5 %	5.5 %	5.5 %	5.5 %	5.5 %	5.5 %	33 %
At 1.85 m of CS inlet	10.8 %	11.4 %	11 %	12 %	13.7 %	13.5 %	72.4 %
At 1 m of CS inlet	9.1 %	10.0 %	10.4 %	11.9 %	10.3 %	9.7 %	61.4 %
At 0.85 m of CS inlet	9.2 %	9.4 %	14.5 %	9.7 %	8.9 %	10.1 %	61.8 %
At 0.41 m of CS inlet	8.9 %	9.3 %	8.2 %	10.1 %	9.5 %	9.1 %	55.1 %

## DEVELOPMENT OF THE BONDED TAILS OF THE PF COIL WINDINGS

### Design

The ITER PF coils design consists of a stack of double pancakes of cable-in-conduit conductor with a square section jacket. At each joint and terminals of a double-pancake, a structural element is required to transfer the hoop force from the outmost conductor to the winding-pack. The design envisages a ‘tail’ welded to the terminal conductor jacket, bonded to the adjacent turns, transferring this force by shear through the interposed insulation to the winding pack. A design was developed in the framework of contract EFDA00-541. The scope of the present task is to design and build a mock-up, representative of the main features of the coil tail and to subject it fatigue cycled test, at  $\text{LN}_2$  temperature, at ENEA laboratory (Brasimone, Italy).

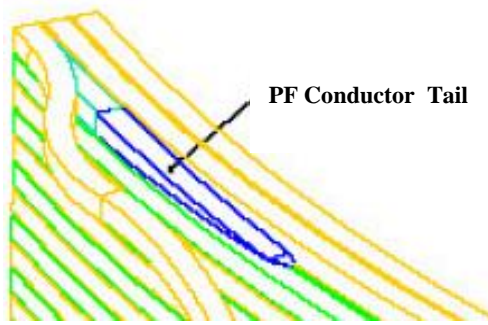


Figure 3: PF coil tail from ITER drawing  
FEAT-1201690003

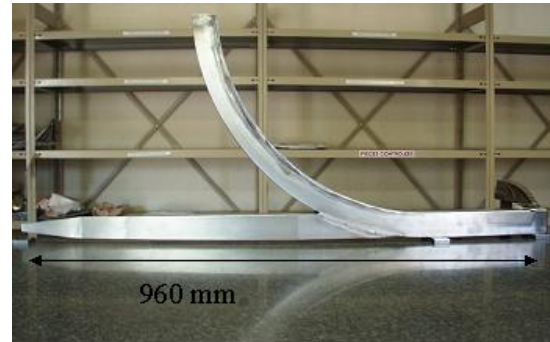


Figure 4: Coil-Tail mock-up, welded onto conductor jacket on the terminal bend

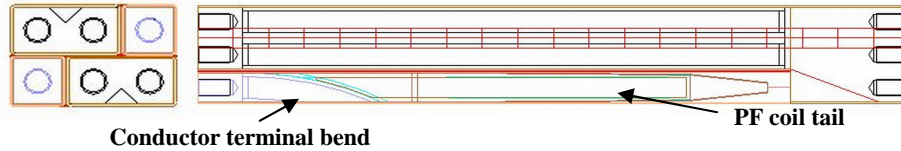


Figure 5: Overall view of the mock-up design

**Manufacturing of mock-up and tests structure**

The manufacturing of the coil tails parts and the adjacent steel plates was completed in 2005. The assembly and impregnation of the mock-up was performed by Alstom under CEA specifications. The insulation wrapping, according to the ITER design, consisted of various layers of coupled glass-fibre/Kapton, half overlapped. Particular attention was paid to the filler parts, machined from special high glass density G10 material (Micam®) to limit thermal induced stresses at cool-down. Following impregnation, the end faces of the mock-up were machined to provide smooth surface to assemble the bolted flanges, anchoring the mock-up to the test structure. Finally dielectric high voltage tests at 4.5 kV were performed to confirm the insulation integrity.

To overcome the strict space limitations and apply sufficient pre-load (400 kN per bolt), special bolts M30 bolts, in Inconel 717, were procured (PS-Superbolt®), and a special test structure, required to invert the test machine compressive force into traction force on the mock-up, was also designed and manufactured. The latter consists of two coaxial tubes and flanges, 100 mm thick, where the mock-up end faces are bolted.



Figure 7: Mock-up fully assembled with test structure ready for transport



Figure 6: PF tail mock-up after impregnation and end face machining

The bent conductor jacket were extracted and subjected to tensile cycled testing at 7K, at the FZK laboratory. The weld test samples were able to withstand 60000 cycles at an equivalent tensile stress of 400 MPa (average on the sample section) and would fail after 22000 cycles at 500 MPa. The expected result was that the sample would pass the 60000 cycles at 600 MPa. Further investigation showed a not complete penetration of the weld explaining the results. This is not considered satisfactory as a full qualification of the weld to be implemented on the ITER-PF. As similar welds were performed on the coil-tail mock-up parts, the load level for cycle testing the mock-up was reduced from twice the nominal load to the nominal load. This does not meet the requirement of a full qualification of the process, nonetheless a successful test at the nominal load and 60000 cycles would provide invaluable experience and source of data. Given the limitations of the computing codes in cases of stresses are in bonded surface, it could provide an experimental confirmation, and confidence, on the sound basis of the design.

**Tests on the mock-up**

The fatigue cycled tests, of the mock-up, at LN<sub>2</sub> temperature, took place at ENEA Brasimone in February 07. In preparation of the tests, optical targets and cameras were installed to measure displacements at two symmetric locations. Temperature sensors mounted at various levels on the test structure to monitor the cooling down phase. The mock-up and test structure were inserted in thermally insulated steel vessel. Thick glass/epoxy blocks were used for insulating the vessel bottom and the top plate of the mock up test structure from the machine piston. To maintain the piston always in contact, considering the piston friction of 120 kN, a minimum load was set at 140 kN. Cycling was between 1400kN and 140 kN with 10 seconds periods (faster operation was attempted, but found not to be compatible with the overall piston movement of about 4 mm). Recording of data was set at 4 Hz. Cool-down took 7 hours to fill-up the vessel with LN<sub>2</sub>. Few hundred cycles were performed at half load to verify for linearity, immediately followed by the 60000 cycles at full load, which lasted for 6 days. The recorded optical measurements on the mock up were unchanged over the 60000 cycles and show linearity with the cycles at half load. The measured displacement of 2 mm peak to peak is consistent with the estimates of 1 mm displacement on the mock-up plus 1 mm deflection in the test structure. The final analysis and assessment of data is underway but the indications are that the mock-up passed the test successfully.



Figure 9: Test machine and LN tank during cycled tests

**CONCLUSIONS**

This task is devoted to design and fabrication of mock-ups for three different items: the TF helium inlets, the CS helium inlets and the PF bonded tails. During the year 2006, the task was terminated by the following actions: A final report on the work on the TF inlets terminated in the previous year was issued [1].

For the CS inlet, it was agreed to stop the mechanical qualification due to the lack of relevant material for conductor manufacture. An hydraulic qualification mock-up manufactured in 2005 using a TFMC type cable with square steel jacket was tested for hydraulic characterisation. The pressure drop was found very low and equal to the conductor unit length. All the petals were found over cooled at every distance of the inlet. A final report was issued [2].

The manufacture of the PF tail mock-up was terminated in year 2006. The final report was issued [3]. The testing of the mock-up concludes the activity, for the PF coil tail development undertaken in the task framework. Unfortunately, due to problems in the welds between ‘tail’ and conductor, which can be overcome, the tests at nominal conditions were then cancelled in agreement with EFDA. A full qualification at twice the full stress load was not possible. However the tests undertaken at nominal load have demonstrated the sound basis of the design. For a full qualification at twice the nominal load new mock-up would be required.

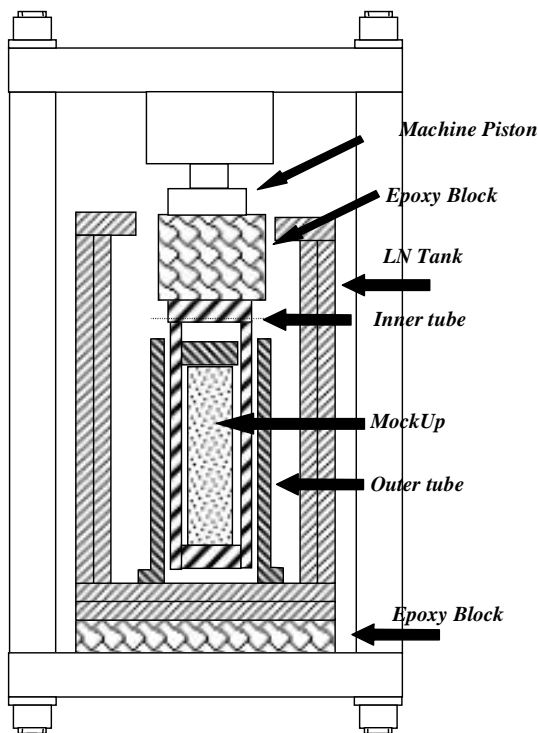


Figure 8: Schematic of the test set-up with the PF tail mock-up, test structure and test machine

## REPORTS AND PUBLICATIONS

---

- [1] P. Decool, H. Cloez, S. Nicollet, J.P. Serries, EFDA contract 03-1015 – Deliverable 2: Final report on TF cooling inlet mock up manufacture and test, CEA internal report AIM/NTT/2005.024, 05/04/2006
  
- [2] P. Decool, H. Cloez, EFDA contract 03-1015 – Deliverable 4: Final report on CS cooling inlet mock up manufacture and test, CEA internal report AIM/NTT/2006.021, 27/07/2006
  
- [3] N. Dolgetta, EFDA contract 03-1015 – Deliverable 6: Final report on the Development of the bonded tail of the PF coil windings, CEA internal report AIM/NTT/2006.013, 04/07/2006

## TASK LEADER

---

Patrick DECOOL

DSM/DRFC/STEP  
CEA-Cadarache  
F-13108 Saint-Paul-lez-Durance Cedex

Tel. : 33 4 42 25 43 50

Fax : 33 4 42 25 26 61

e-mail : [patrick.decool@cea.fr](mailto:patrick.decool@cea.fr)

---

## Task Title: TW4-TMSC-SAMAN1: MANUFACTURE OF SUBSIZE SAMPLES

---

### INTRODUCTION

---

The tests of the ITER TF model coil in 2001 – 2002 have shown that the performance of the conductor was lower than expected. New high performance strands have been ordered by EFDA to industry.

In the framework of the SAMAN task, EURATOM-CEA Association has to explore the sensitivity of these high performance Nb<sub>3</sub>Sn strands on stainless steel jacketed subsize samples, regarding the critical properties. This will be done by ordering and manufacturing subsize samples in the industry and then by participating in the tests at FZK (Germany) in the FBI test facility, and in their interpretation.

In the first stage of the scientific program, using OST strands, subsize cables of different cable layouts (9, 45 and 180 strands) have been produced, the number of pure copper strands the void fraction or the cabling pattern, have been varied.

In the second stage of the saman task, strands originated from different companies will be tested on two kinds of subsize samples such as to compare the sensitivity of the different strands to the strain. A first strand manufactured by OCSI has been tested in the FBI test facility. An analysis of the results is presented.

### 2006 ACTIVITIES

---

#### OBSERVATION OF STRAIN DEGRADATION IN SAMAN SAMPLES OF THE FIRST STAGE

##### Increasing the Lorentz force in FBI by testing the samples a low field down to 10 T

Starting from the test of the model coils of ITER and especially from the ITER TF model coil, it has been demonstrated that the Lorentz force, due to the combination of the high transport current in the cable and of the high magnetic field surrounding the conductor, has clearly an effect on the critical properties of the strand. What is not still completely clear is whether this effect is due to the global Lorentz force on the sample or whether it is due to the Lorentz force acting on each individual strand by bending them or whether both of them are playing a role in a complex form.

Lorentz force per strand in ITER TF system (11.8 T, 68000 A, 900 superconducting strands): 892 N.

The FBI test facility is operating only at 4.2 K. Due to the technology of the connection and due to the test procedure (inductive mode), it is assumed that the current distribution

among the strands is homogeneous. FBI offers two ways to increase the Lorentz force, which increases the strain in absolute value, and enables to observe the effect on the samples:

- The first way is to stretch the sample by pulling on it, which uncompresses the sample and decreases the strain (in absolute value). The critical properties of the sample are therefore improved simultaneously with the Lorentz force increase, and the process can reveal different behaviors according to the sample properties. This is the classical way of using the FBI test facility which can provide in addition, at maximum performance, the initial compression of the sample due to heat treatment. The results of these tests have been presented in a recent paper.
- The second way is, before stretching the sample, to explore the sample critical properties at different fields using the maximum capacity of the FBI power supply (10 kA). Contrary to what is generally thought, the maximum of Lorentz force is reached not at high magnetic field but at low magnetic field (the minimum field practically applicable in FBI is 10 T). The results of this approach are reported here.

Using the second way, the order of magnitude of the Lorentz force in FBI is far above the nominal Lorentz force in ITER TF system (by around three times). It is therefore very interesting to investigate the effects on critical current of such tests at low field.

#### The detrimental effect of the Lorentz force on samples

Classically, from the critical current measurement at given field and temperature (B and T=4.2 K), and taking into account classical correlations for  $J_{noncu}$  as a function of B, T and  $\epsilon_{effective}$  (the strain), an effective value of the strain, can be deduced.  $S_{noncu}$  is the non copper section in the strand.

$$I_c = S_{noncu} J_{noncu} (B, T, \epsilon_{effective})$$

The detailed results of this study have been published in [1].

It is illustrated in figure 1 where two samples with the same number of OST type 1 strands (30 superconducting strands and 15 copper strands) have been tested at different magnetic fields. Figure 1-a regards sample n05 with 25 % void fraction, while figure 1-b regards sample n06 with 45 % void fraction. The typical Lorentz force per strand is 1400 N/m at 14 T (already larger than in ITER) and 2200 N/m at 10 T. The behaviour of sample n05 shows better resistance to strain degradation to Lorentz force including a region with a plateau.

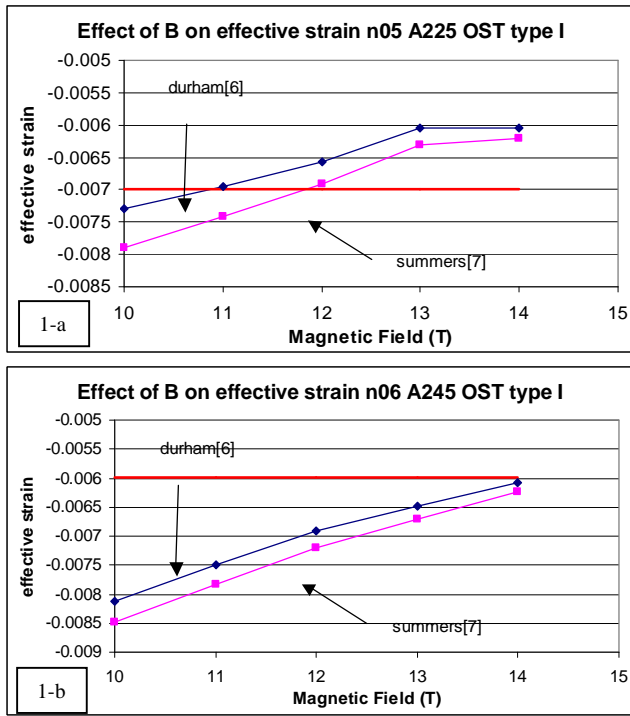


Figure 1: Effect of field on strain degradation for two different OST type 1 samples during first stage of the scientific program (effect of void fraction)

- The main conclusion of this study is that the strain degradation is already visible on small subsize samples (45 strands) showing that the Lorentz force per strand is probably playing a major role.
- OST type 1 strand strands behave better sans OST type 2 showing the role of the strand.
- Subsize samples with low void fraction (25 %) showed better performance and less sensitivity to strain than samples with high void fraction (45 %) or samples with standard void fraction.
- Subsize samples with long twist pitches (45 mm/85 mm/125 mm) showed better performance than samples with small twist pitches (35 mm/ 65 mm/110 mm).

**High Lorentz force during Sultan tests on full size conductor?**

It is well known that the contact resistances of the strands constituting the cable with the copper sole of a connection such as the one equipping the Sultan full size sample, are far from being homogenous. At given field, the current is increased in the sample and in this inductive phase the current can be relatively well distributed within the strands because it is inductively driven. After a short relaxation time, which can be in the order of few minutes in Sultan, the current distribution relaxes to a resistive mode where the current in certain strands is probably very high and limited only by its critical value. In these conditions the Lorentz force can be very high especially at low field. The paradox is that, at low field, the samples can be severely damaged by hidden large currents circulating in the strands connected by the lowest contact resistances. The tests in FBI have shown that the tests at low field are associated with the largest Lorentz forces and therefore the largest effective strains (in absolute value). Careful examination of the sequence of tests at Sultan or on the

dipole prototype conductors can reveal that tests at low field are particularly degrading the conductor. Note that the relaxation phase in ITER TF system will probably take, due to the long length of conductor, more than one hour.

**SAMPLES OF THE SECOND STAGE OF THE SCIENTIFIC PROGRAM**

In the second stage of the saman task, several strands from different companies are planned to be tested, to explore their sensitivity to strain. All the samples related to this second stage have now been manufactured. The results presented here are related to an OCSI strand. The particularity of the OCSI strand is that the copper to non copper ratio is high: 1.5. The characteristics of the strand are the following: Billet number: NS026001  $J_{noncu}(12T, 4.2 K, 0) = 1030 A/mm^2$ . The detailed results of this study have been published in [2].

It is illustrated in figure 2 where two samples with the same OCSI strand and same standard void fraction have been tested at different magnetic fields. Figure 2-a regards sample n31 with 30 superconducting strands and 15 copper strands, while figure 2-b regards sample n33 with 60 superconducting strands and 120 copper strands.

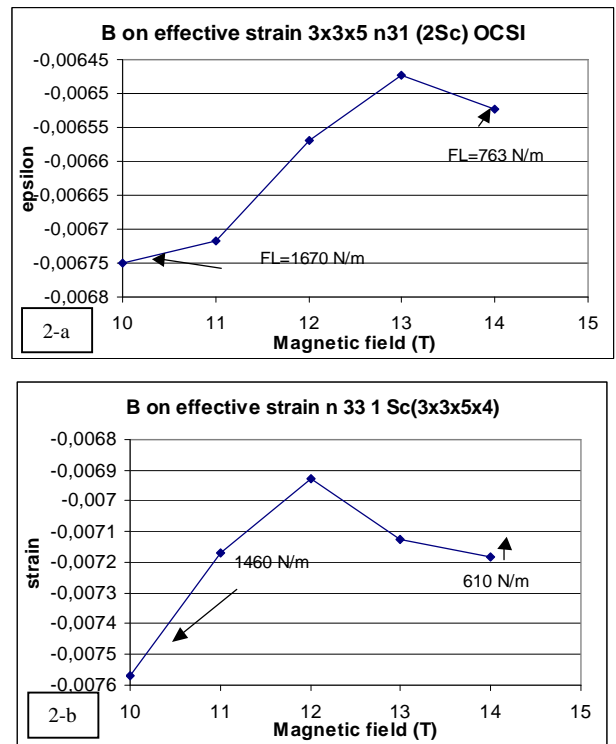


Figure 2: Effect of field on strain degradation of two different OCSI samples during second stage of the scientific program (effect of sample size)

As observed for OST strands, the strain is very correlated to the Lorentz force per strand. The behaviour between n31 and n05 is different because the Lorentz force per strand is smaller due to the high copper ratio within the strand and therefore the strain degradation is smaller for n31 as the field decreases. The influence of the size of the sample is also visible between n31 and n33, showing that the global Lorentz force is playing a role an not only the Lorentz force per strand.

### Is there an interest for ITER TF coils to high copper ratio strands like OCSI strands?

At given Lorentz force per strand, the OCSI strand is not far better than the OST strand. However we cannot consider that the four legs of the EU TF-AS samples recently tested in Sultan [3], were operated at the same Lorentz force per strand.

Supposing the current perfectly distributed among the strands at given sample current, due to the number of superconducting strands in the cable, the Lorentz force was smaller by 50 % in the OCSI leg than in OST leg of the EU TF-AS samples, which makes a big difference.

In addition, it is probably due to current distribution in the conductor, especially at low field, that in some modes, large currents can be induced in some strands producing large Lorentz force in the strand.

With respect to this behaviour, OCSI strands due to lower non copper section, at same non copper current density as in OST strands, provide a kind of auto-limitation of the induced current by about 50 % lower than in OST strands. This can explain the good results of the OCSI leg in the EU TFSAS samples which provided the best Tcs of the four legs, not far from ITER requirement and especially with nearly no degradation by cycling (contrary to OST and OKSC samples), which is very safe for the designer.

This behaviour confirms what has been observed with such a strand in the TFMC and in the associated Sultan samples.

It cannot be stated that the Lorentz force per strand is the only driver of the degradation due to strain and it is confirmed that the total Lorentz force per conductor is also playing a role.

Again there is now an interest to test the FBI samples by cycling them at different Lorentz forces as proposed in [1].

## CONCLUSIONS

---

To reduce the average Lorentz force and prevent as far as possible hidden local Lorentz forces, is certainly determining.

There are several ways to go to this direction:

- By not choosing very advanced strands in the project, which by definition can accept in them very high current and associated very high Lorentz force. The very advanced strands are famous to be more fragile than the non advanced strands but they have certainly also this faculty to auto damage themselves by accepting "naturally" high Lorentz forces.
- By spreading non copper in the overall section and suppressing copper segregation (but this solution has a high cost).
- By improving the strand support either by decreasing the void or by improving the twist pattern. Samples with long twist pitches have proved to behave better during the FBI tests.
- The inhomogeneous current distribution within a petal, which was supposed not to affect the conductor performance, thanks to current redistribution in the high field zone, is eventually an issue due to hidden high

Lorentz force. A reflexion has to be carried out to improve this current distribution in joints.

## REPORTS AND PUBLICATIONS

---

- [1] J.L. Duchateau, N. Dolgetta "EFDA contract TW4-TMSC-SAMAN1: "Second intermediate report Estimation of the detrimental effect of Lorentz forces on Nb<sub>3</sub>Sn strands by critical current measurements in the FBI test facility" October 2006 internal CEA report AIM/NTT-2006.032
- [2] J.L. Duchateau, N. Dolgetta "EFDA contract TW4-TMSC-SAMAN1: OCSI strand" December 2006 internal CEA report AIM/NTT-2006.040
- [3] D. Ciazynski, "Review of Nb<sub>3</sub>Sn conductors for ITER". Presented at the 24<sup>th</sup> SOFT Conference September 2006 (Warsaw, Poland)

## TASK LEADER

---

Jean-Luc DUCHATEAU

DSM/DRFC/STEP  
CEA-Cadarache  
F-13108 Saint-Paul-Lez-Durance Cedex

Tel. : 33 4 42 25 49 67

Fax : 33 4 42 25 26 61

e-mail : jean-luc.duchateau@cea.fr

**CEFDA04-1170**

---

**Task Title: TW4-TMSC-RESDEV: DEVELOPMENT AND TESTING ON NEW RESIN SOLUTION**

---

**INTRODUCTION**

---

New advanced cyanate ester-based resin materials have been tested and found to have significantly improved radiation resistance as compared to currently used resins. Therefore, it is necessary to stimulate the activity within Europe to gain experience with these new resin systems in close collaboration between the associations and the European companies.

The primary objective of this task is to industrialise the vacuum impregnation technique of new advanced resins with optimised catalyst contents, resin temperatures and lifetime for large magnet systems. To qualify the process, a mock-up with about 50 kg of resin will be manufactured.

**2006 ACTIVITIES**

---

The work with Hunstman has continued to find a resin formulation which fulfils the requirements for an impregnation process. The baseline was a 40/60 CE/epoxy blend. At the end of November 2006, a formulation has been proposed which shows a pot life of 24 hours and a suitable viscosity profile; if the curing at 150°C is not complete, the degree of curing is similar to the degree measured on samples tested positively by ATI, so we can expect similar mechanical behaviour. The safety studies have begun.

Following the conclusions of the mechanical studies after irradiation made at ATI on different CE/epoxy blends, EFDA has decided in March 2007 to change the baseline from the 40/60 to the 30/70 CE/epoxy blend as baseline. So a new campaign of tests has to be done to correct the amount of catalyst, check the viscosity profile and the curing conditions.

**TASK LEADER**

---

Françoise RONDEAUX

DSM/DAPNIA/SACM/LEAS  
CEA-Saclay  
F-91191 Gif-sur-Yvette Cedex

Tel. : 33 1 69 08 64 49

Fax : 33 1 69 08 69 29

e-mail : francoise.rondeaux@cea.fr

## Task Title: TW4-TMSC-CRYOLA: CRYOGENIC TESTS ON ITER MAGNET STRUCTURAL MATERIALS

### INTRODUCTION

The main objective of the task was:

- To perform cryogenic tests at 4 K, 77 K and room temperature to characterize the structural materials of the ITER magnets from the thermal and mechanical point of view (e.g.: jacket, TF case, ...);
- To spread and standardize the available know-how on this type of cryogenic tests across the European laboratories to be prepared for the large number of tests necessary during the ITER magnet procurement action.

This task is performed in collaboration with FZK for the definition of the standard procedures to be followed during mechanical cryogenic tests at 4 K, 77 K and room temperature.

Air Liquide / DTA and CEA / SBT have been collaborating for years in the field of material characterization: Air Liquide / DTA is in charge of Mechanical tests (Young modulus, tensile tests, compression tests, fatigue tests ...) while thermal tests are performed at CEA / SBT (thermal expansion, thermal conductivity ...).

From a technical point of view, the work is separated in two parts: the first one concerns the upgrade of the test benches to improve the quality of the measurements and to standardize the measurement procedures (especially for mechanical tests).

In the second part, the same tests were carried out at the FZK laboratory and at CEA / SBT and Air Liquide / DTA. Then the results were compared.

After all these tests a preliminary study was done concerning the time scales and the requirements in terms of equipment versus number of tests per year needed for the ITER quality program of the magnets.

This task started at the beginning of 2005 and was finished at the end of 2006 [3].

### 2006 ACTIVITIES

#### THERMAL TESTS:

In 2005, all the thermal tests of the contract were performed for the stainless steel and composite samples. After some difficulties in 2006 for the elaboration of the material foreseen in the RESDEV task, the thermal tests on these samples have been postponed.

### MECHANICAL TESTS

About the mechanical tests, the year 2005 was dedicated to the update of the test bench to be able to perform fatigue tests. In 2006, these tests have been done.



Figure 1: Mechanical test bench

### FRACTURE TOUGHNESS

Such a test was performed on aluminium 7020 material following the E399 standard at room temperature. The measurements and some samples after tests are shown on figures 2 and 3.

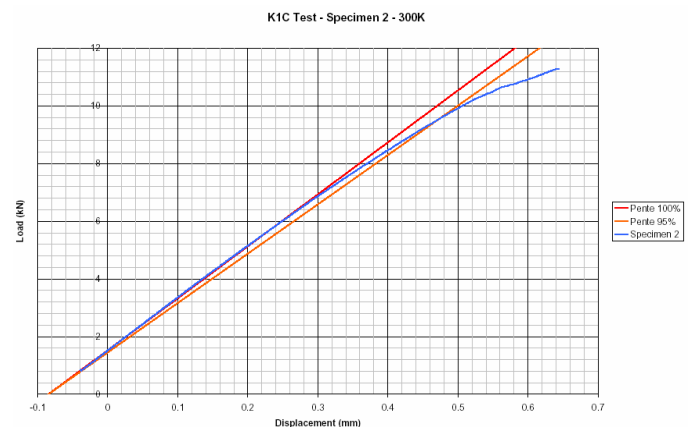


Figure 2: Load - Displacement Diagram allowing to calculate the Fracture toughness

A good agreement was found between FZK ones and our measurements.



Figure 3: Aluminium 7020 specimen after fracture

**J-TEST**

The test campaign using an automatic load ramping gave good quality results. The tests were performed with stainless steel samples (grade 316 LN) at 4 K. The results for one measurement are given in figures 4 and 5.

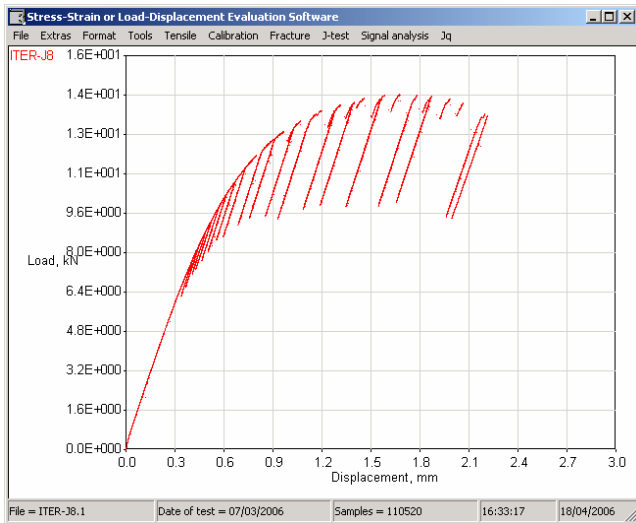


Figure 4: Load displacement diagram for 316 LN

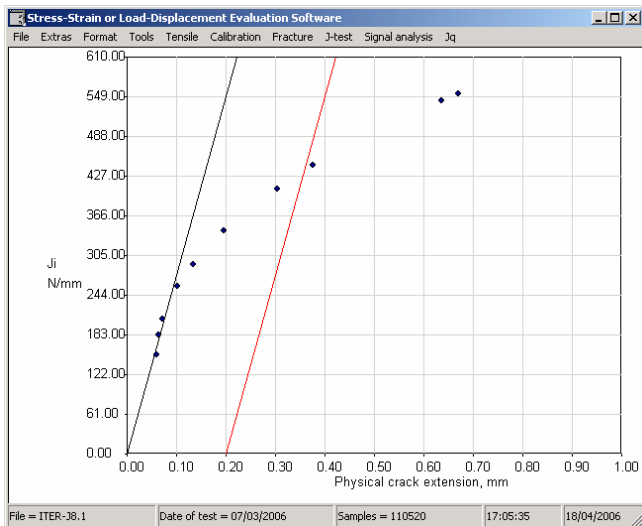


Figure 5: Diagram for  $J_Q$  determination

As for fracture toughness, a good agreement with the FZK measurements was found.

**FATIGUE CRACK GROWTH RATE TEST (FCGR)**

These tests were performed on stainless steel material (grade 316LN) at 4 K. An up-to-date procedure, from FZK was applied for these measurements and the analysis done by Air Liquide showed a good understanding of the method.

Figure 6 presents the results of this measurement.

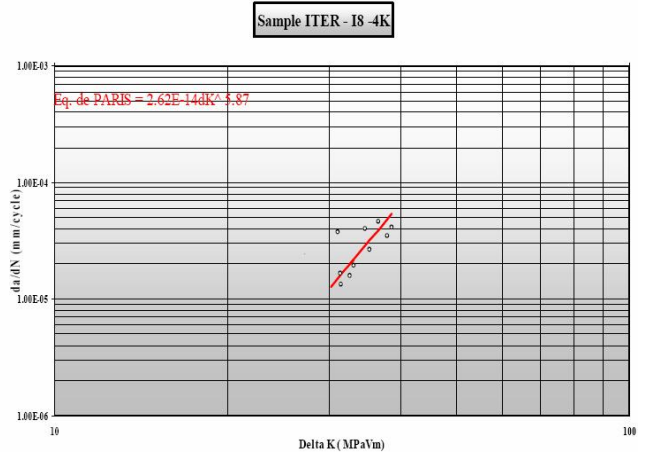


Figure 6: FCGR test

**DEVELOPMENT OF TEST BENCHES**

As only few inputs are so far available in Europe concerning the amount of tests needed for the magnet ITER quality program, different assumptions and scenarios were taken into account for mechanical and thermal tests. The table 1 summarises the result of this study according to the test type.

Table 1: Tests required for Iter magnet quality program

Mechanical tests	Up to 50 tests/year	Nothing required
	From 50 to 250 tests/year	Automation of the current test benches (delay: 6 months)
	Beyond 250 tests/year	Test bench dedicated to ITER program needed (delay: 12 months)
Thermal expansion coefficient	Up to 50 tests/year	Nothing required
	Above 50 tests/year	Additional test bench(es) dedicated to ITER program (delay: 12 months)
Thermal conductivity	Few tests/year due to the needed time for one test (10 days)	New test bench is envisaged to reduce the effect of radiation near the room temperature (delay: 14 months)

**CONCLUSIONS**

Concerning thermal tests (coefficient of thermal expansion and thermal conductivity), the high skill already present at FZK and CEA / SBT in this field resulted in a good agreement between all the measurements.

Concerning mechanical tests, Air Liquide was able to perform standard tests in good conditions and nothing special was required. For the fatigue tests, FZK transmitted the skill to Air Liquide and the measurements performed then and analysed by FZK showed that they were properly carried out by Air Liquide. This validates the capability of Air Liquide to perform these types of tests.

Because of lack of input data from Europe and / or ITER team so far, concerning the number of tests per year, different assumptions were envisaged to estimate the necessary developments to be carried out in order to be able to face the ITER Magnet quality program.

## REPORTS AND PUBLICATIONS

---

- [1] Minutes of meeting: third intermediate meeting on April 26<sup>th</sup> 2006 – CEA internal report SBT / 06-115 / JMP
- [2] Second intermediate report for CRYOLA task (phase 4 to 8) – Note SBT/CT/06-58 – September 2006
- [3] Final report to the contract FU06-CT-2004-00181 (EFDA / 05 – 1215) between the European Atomic Energy Community and Euratom / CEA Association About – Note SBT/CT/06-83 – December 2006

## TASK LEADER

---

Alain GIRARD

DSM/DRFMC/SBT  
CEA-Grenoble  
17, rue des martyrs  
F-38054 Grenoble Cedex 9

Tel. : 33 4 38 78 43 65  
Fax : 33 4 38 78 51 71

e-mail : [alain.girard@cea.fr](mailto:alain.girard@cea.fr)

**CEFDA04-1219**


---

## **Task Title: TW4-TMSC-SAMFSS: MANUFACTURE OF TWO FULL SIZE SAMPLES OF Nb<sub>3</sub>Sn STRANDS**

---

### **INTRODUCTION**

---

Following the revision of the design of the ITER TF conductor in 2003, relying on the use of advanced Nb<sub>3</sub>Sn strands, EFDA launched an R&D programme in 2004 to procure advanced strands in industry. The final advanced Nb<sub>3</sub>Sn strand qualification will be done by the testing of two full size conductor samples. This task covers the manufacturing of the samples according to the requirements of the SULTAN facility. The work includes the joint fabrication, sample assembly and instrumentation. The manufacture of the conductor lengths is performed by ENEA and the heat treatment is performed at CRPP (Switzerland). The zero field joint resistance will be less than 2 nΩ, in order not to interfere with the conductor measurements. The same applies to the upper terminations, which will meet the CRPP/SULTAN requirements. The two full-size samples (corresponding to four legs) will be made using different types of advanced strand.

### **2006 ACTIVITIES**

---

#### **PREVIOUS ACTIVITIES**

The sample design was defined in year 2005. The first sample EU-TFAS1 was manufactured at Ansaldo Superconduttori (A.S., Italy) under CEA monitoring and was delivered for test in the CRPP/SULTAN test facility in November 2005.

The manufacture of the second sample using OKSC and OCSI conductors has started in September 2005. The two legs were sent for heat treatment to CRPP in November 2005 and sent back to A.S. in December 2005 for final sample assembly.

#### **EU-TFAS2 MANUFACTURE**

The manufacture of the sample started in September 2005. This sample uses the OKSC and OCSI conductors.

The preparation of the two legs was done in the same way as described for the first sample. After the heat treatment at CRPP, the two legs were back to A.S. for final assembly in January 2006. The final assembly was performed in the same way as it was performed for the first sample. The geometry, tightness and electric insulation were checked to be in accordance with the specifications. To save time, it was agreed to perform the final instrumentation in the CEA laboratory, the sample was then delivered to CEA-Cadarache on March 2006. From the experience gained on the test of the first sample, it appears that the thermalization of the temperature sensors was not correct. So, all the instrumentation was identical to the first sample

excepted the temperature sensors which were assembled with an additional thermal insulation. In addition, the temperature sensors were doubled in the high field region using remaining CERNOX sensors with a layout identical to the one successfully tested on the old full size samples (SS-FSJS and PF-FSJS). The final delivery to CRPP for tests was in April 2006 (figure 1).



*Figure 1: The EU-TFAS2 ready to be sent to CRPP for test*

### **CONCLUSIONS**

---

The task SAMFSS is devoted to the manufacture of two full size samples to be tested in the CRPP test facility. These samples were designed with a TFMC type conductor using circular steel jacket. Each sample uses two conductor lengths each of them using one candidate advanced strand proposed by the industry. Four different strands will then be tested in the same cable configuration and the results will be compared to the previous results gained on the TFMC full size joint sample. The production of conceptual drawings and the manufacture were performed by Ansaldo Superconduttori (Italy) and started in May 2005. The first sample was manufactured with EAS and OST strands and delivered to CRPP for tests in November 2005. In the same time, the second sample manufacture was started after delivery of the conductors using OCSI and OKSC strands in September 2005. After preparation of the two sample legs and heat treatment at CRPP, the legs were back to A.S. in January 2006. The final assembly was performed in the same way as it was performed for the first sample. After the final dimensional, tightness and insulation tests, it was decided to send the sample to CEA-Cadarache for instrumentation. The temperature sensors which were detected after the first sample test to be incorrect were modified and doubled in the high field region to insure a better temperature measurement. The final delivery to CRPP for tests was in April 2006. A final report was issued

[1]. This last sample concludes the task with the two samples set which are the first which could give helpful information on the performances of advanced strands for ITER TF magnets in real cable-in-conduit conditions.

## **REPORTS AND PUBLICATIONS**

---

[1] P. Decool, H. Cloez, N. Dolgetta, P. Libeyre, J.L. Maréchal, J.P. Serries, Contract EFDA 04-1219: Deliverable 3, Final report on the Full-Size Sample manufacture, CEA internal report AIM/NTT-2006.019, 07/06/2006.

## **TASK LEADER**

---

Patrick DECOOL

DSM/DRFC/STEP  
CEA-Cadarache  
F-13108 Saint-Paul-Lez-Durance Cedex

Tel. : 33 4 42 25 43 50  
Fax : 33 4 42 25 26 61

e-mail : [patrick.decool@cea.fr](mailto:patrick.decool@cea.fr)

**Task Title: TW6-TMSC-THCOIL: THERMOHYDRAULIC ANALYSIS FOR THE ITER SUPERCONDUCTING COILS**

**INTRODUCTION**

In the framework of the thermohydraulic analysis for ITER superconducting coils, the main objective of this task is to provide assistance to the ITER International Team in performing thermohydraulic simulations of the ITER TF coils for a range of operating scenarios and parametric analysis. This analysis allows to update the conductor design documentation and to investigate the impact of selected design parameters on the conductor performance and the cooling loop efficiency.

The CEA and the D.V. Efremov Scientific Research Institute of Electrophysical Apparatus have signed a cooperation agreement for the utilization of the VINCENTA software developed by Efremov Institute. This cooperation concerns, inter alia, the use of the VINCENTA code for the modelisation of the ITER cryogenic system. All the results presented here were derived with the vincenta code.

**2006 ACTIVITIES**

**TF COIL MODEL DESCRIPTION**

The ITER 18 TF coils are “D” shaped and consist of a winding pack contained in a thick stainless steel casing. The TF Winding Pack (TFWP) is included in a structure of radial plates (which contain the conductor), with an outer insulation. The casing surrounds completely the winding pack and is closed by welding. A cross- sectional view of the TF coil model is shown in figure 1. Figure 2 shows the layout of cooling inlets/outlets and the positions of the cross-sections considered in the calculation.

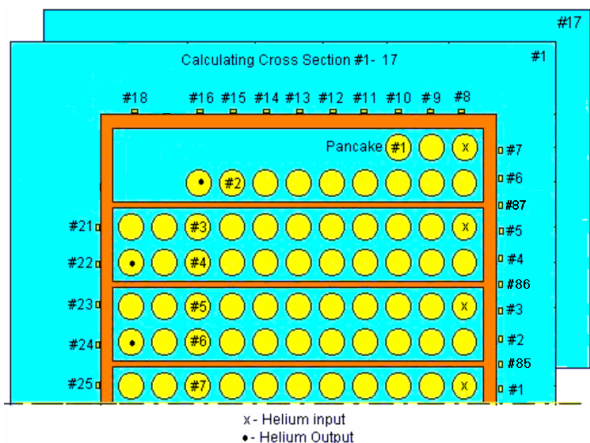


Figure 1: Geometry of the coil cross-section (conductors are in yellow color)

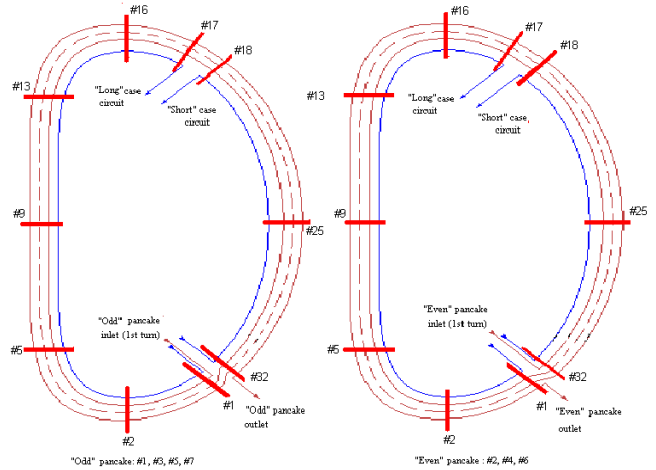


Figure 2: Layout of the He inlets/outlets and cross sections

**CRYOPLANT CONTROL DESCRIPTION**

Usually, a helium cryorefrigerator is operated in steady state with mixed operation including constant refrigeration and liquefaction capacities. Therefore, in the particular case of ITER, variable heat loads which are induced by the magnet system itself and the nuclear heating, must be smoothed before reaching the cryoplant.

The ITER cooling system consists of two main loops (see figure 3) cooled by a forced flow of supercritical helium: one loop cools the casing and one loop cools the TF winding pack. Each loop includes a circulating pump and all the heat deposited in the loop flows to the heat exchanger.

Two other loops dedicated to the central solenoid (CS) and the poloidal field (PF) have also to be considered, as they contribute to the total heat load to the cryoplant, as it can be seen on figure 3. These cooling systems are considered in the analysis by the time-dependent heat deposited into the bath of the heat exchanger. In the analysis only 1 bath instead of four in reality are considered. This bath receives all the heat deposited in the structures and the different magnetic systems.

*Heat Load into the helium bath*

The smoothing of the total heat load is performed through the control on the heat loads coming from the TF casing circuit only. When the variable heat load coming to the saturated bath tends to increase over its average value, part of this load coming from TF case is derived and will be released after the plasma pulse, when the loads to the bath will decrease. To achieve this, a cooling scheme with a by-pass valve is used. Indeed, two control valves are considered in the casing cooling loop.

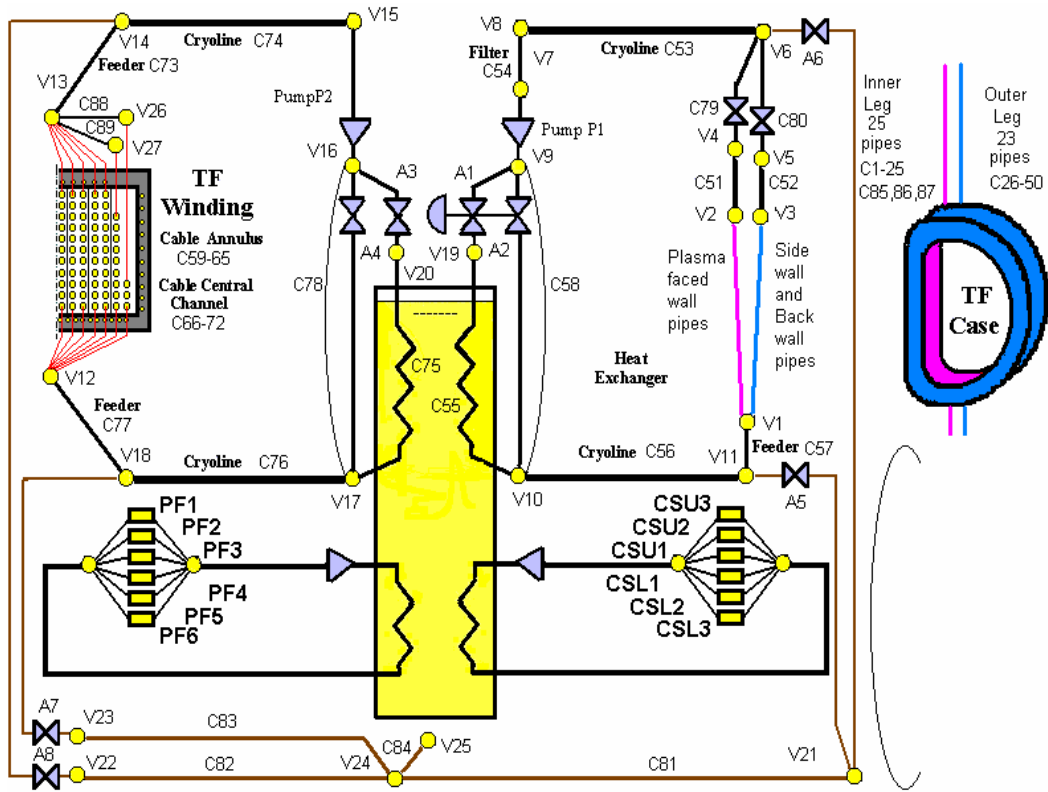


Figure 3: Four Cooling loops: above TFWP and Casing loops, below CS and PF loops

The total cross-section of the system of valves (control + by-pass) seen by the helium flow remains constant, so that the circulating pump always operates on the same characteristic point. When the instantaneous sum of the heat loads from all the magnet systems transferred to the cryoplat becomes higher than its average value, the by-pass valve of the TF casing cooling circuit is opened and only one part of the total supercritical helium flow reaches the heat exchanger. So, the temperature of the structures increases. The temperature of the structures is allowed to vary in a larger range than the coil temperature.

**Parametric study**

Different ITER plasma scenarios were studied:

1. Reference plasma scenario: 15 MA plasma, 500MW, 400 s burn
2. Reference plasma scenario: Plasma disruption at end of burn 7th pulse
3. Hybrid scenario: 14 MA plasma, 400 MW, 1000 s burn
4. High nuclear heating scenario: 17 MA plasma, 700 MW, 200 s burn

We studied the sensitivity to the main **thermo-hydraulic parameters** (mass flow rate for casing loop, bath

temperature for heat exchanger...) and the **sensitivity to changes in conductor parameters** in order to verify that the magnet system always remains in the superconducting area (the value of electrical field should be less than 2  $\mu$ V/m).

**CONTROL PERFORMANCE DURING NORMAL OPERATION OF ITER**

**Simulation without power control**

This simulation is first performed to estimate the total average heat load. The total average heat power over a plasma pulse is 26.1 kW as shown in figure 4.

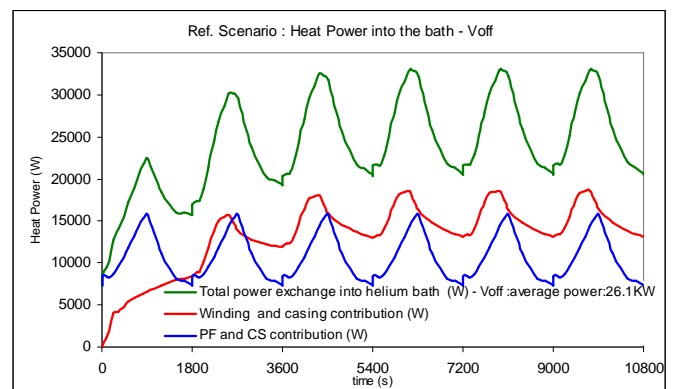


Figure 4: Time evolution of different heat power contributions into the bath

## Simulation with power control

The value for the control of the variable load is chosen to be close to the average heat load calculated from the previous simulation. Each valve aperture is controlled to split the SHe flow between the heat exchanger and the bypass circuit, to ensure that the total heat load on the LHe bath is kept below **the fixed limit**. This limit will be some % higher than the average heat load in order to obtain steady state conditions for strand temperature and electrical field. Figure 5 shows the time evolution of heat power into the bath with two different controls. It appears that the cryoplant control algorithm does not ensure a complete smoothing of the pulsed heat load.

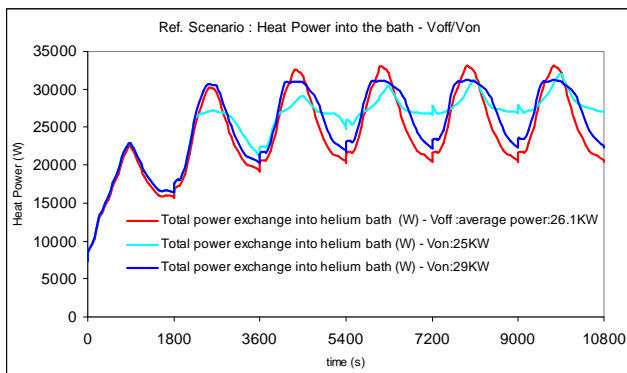


Figure 5: Time evolution of heat power into the bath without and with control

## CONCLUSIONS

A Thermal-hydraulic analysis of TF coil with and without control operation including the plasma disruption was performed in this study.

First, we derived, for all plasma scenarios, an electrical field value lower than the  $2 \mu\text{V/m}$ . This criterion is the maximum electrical field allowed at the nominal operating point. The peak value is obtained for the pancake #6 in the high field region. Conductor shows a higher temperature in that region, but stays below the 5.0 K design value.

The control of the power does not induce a strong variation of the electrical field.

Second, the analysis performed shows that the cryoplant control algorithm ensures only a partial smoothing of the pulsed heat load. The relative variation of power in the helium bath is about 40%-45% without control and about 18%-20% with the active control. Nevertheless, the dynamic variation of the helium bath power (upstream of cryoplant) with and without control has practically the same slope in the increase phase  $\sim 20 \text{ W/s}$ .

## REPORTS AND PUBLICATIONS

- [1] THCOIL Intermediate report I. August 2006
- [2] THCOIL Intermediate report II. October 2006
- [3] THCOIL Final report. January 2007

## TASK LEADER

Alain GIRARD

DSM/DRFMC/SBT  
CEA-Grenoble  
17, rue des martyrs  
F-38054 Grenoble Cedex 9

Tel. : 33 4 38 78 43 65  
Fax : 33 4 38 78 51 71

e-mail : [alain.girard@cea.fr](mailto:alain.girard@cea.fr)

**CEFDA05-1370**


---

## **Task Title: TW6-TMSC-TFPRO: ITER TF FULL SIZE PROTOTYPE CONDUCTOR**

---

### **INTRODUCTION**

---

In agreement with the ITER Team, EFDA-CSU Garching has decided to qualify the manufacturing feasibility of the present ITER TF conductor design. To this purpose, three full size TF conductor lengths will be manufactured according to the ITER design, using lower performance Nb<sub>3</sub>Sn strand. Our Association shall follow up the whole manufacturing process and shall procure all required components including the lower performance Nb<sub>3</sub>Sn strand.

The work consists in the following sub-tasks:

- 1) Procurement of Cr plated copper strand and lower performance Nb<sub>3</sub>Sn strand.
- 2) Cabling and jacketing of a dummy conductor length using copper strands.
- 3) Cabling and jacketing of three conductor unit lengths according to the ITER TF conductor specification using lower performance Nb<sub>3</sub>Sn strands.

After writing of a technical specification and corresponding call for tender, the contract was passed with the NEXANS company which have the equipment needed for production of ITER type cables and corresponding jacketing, and a wide range of cabling machines in different factories.

### **2006 ACTIVITIES**

---

#### **PROCUREMENT OF CONDUCTOR COMPONENTS**

During year 2006, the components were procured: central spiral, dummy and superconducting strand, jacket-tubes. A length of 24 m of the central spiral was manufactured by the MECARESSORT Firm (France). This spiral is a 9 mm O.D. with a gap of about 40% as specified by IT. Due to the cost and delay for base material procurement, it was agreed to use AISI 304L instead of the AISI 316L foreseen for this spiral manufacture. The spiral was delivered to our Association on June 2006. It is to be noted that this kind of spiral has "tile" deformation as it was observed on the old spiral productions. It seems difficult to overcome this problem without start from a pre-shaped tape in the opposite direction to the tile deformation.

The tubes for the jacket manufacture was produced by INOXTUBE. A minimum quantity of 100 m of tube was delivered to our Association. Half was delivered to ENEA for their conductor manufacture program as requested by EFDA. The dummy copper strand of 0.81 mm diameter were procured by EFDA. The superconducting 0.81 mm

diameter Nb<sub>3</sub>Sn strand was, was made by ALSTOM. These strands were chrome plated by DURALOY.

### **CABLING AND JACKETING OF CONDUCTOR**

After drafting of the technical specification and the relative call for tender, the contract was awarded to the NEXANS company, which has the type of equipment needed for the manufacturing of ITER type cables and jacketing, and a wide range of cabling machines in various factories. The cabling of sub stages up to the sub-petal stage, with dummy and superconductor strands, was performed at OPTICABLE (B) by the end of year 2006. The final cabling of the petals and the cable is planned to be performed in year 2007 at the NEXANS-CORTAILLOD (CH) factory. The final jacketing being planned to be performed at NEXANS Jeumont (France).

### **CONCLUSIONS**

---

This task is mainly devoted to qualify a new conductor manufacturer which is the European company NEXANS. The work has started by the material procurement and the first cabling stages were performed. The final petal and cable stages as well as the cable jacketing will be completed in 2007.

### **TASK LEADER**

---

Patrick DECOOL

DSM/DRFC/STEP  
CEA-Cadarache  
F-13108 Saint-Paul-Lez-Durance Cedex

Tel. : 33 4 42 25 43 50  
Fax : 33 4 42 25 26 61

e-mail : patrick.decool@cea.fr

## TW1-TMS-PFCITE

### Task Title: POLOIDAL FIELD CONDUCTOR INSERT (PFCI)

#### INTRODUCTION

Within the framework of the ITER project, the EU partner has been asked to manufacture a model coil, called Poloidal Field Conductor Insert (PFCI), to be tested in the JAEA test facility in Naka, Japan. The development, manufacture and testing of the PFCI coil shall support the design of the ITER PF conductors and coils.

The main objective of the model coil tests is to get a complete knowledge and understanding of the behaviour of high current NbTi cable-in-conduit conductors and related joints under operating conditions as foreseen for the ITER Poloidal Field (PF1 & PF6) coils. A conductor representative of the ITER PF1 & PF6 coils was wound in a single layer coil and equipped with a numerous instrumentation composed of inductive heaters, voltage taps, temperature and pressure sensors, strain gauges, etc. The coil fabrication was completed in summer 2006 at Tesla (UK), and, due to the time needed to prepare the ITER CS Model Coil (CSMC) test facility at JAEA, the tests are now planned in 2008.

The coil winding features a square conductor with a NbTi superconducting cable inserted in a thick wall, stainless steel jacket. Superconducting joints are required to connect the coil to the current leads. Another joint is located at an intermediate location in the winding to test an ITER-relevant joint under magnetic field operating conditions similar to the ones foreseen in the ITER PF coils. The upper and lower terminations shall connect the winding to the existing CSMC Insert busbar system of the CSMC facility, as well as to the cryogen supplies.

The work of our Association within task PFCITE covers the following items:

- Participation to definition and review of the test procedure
- Participation to operational campaigns of the PFCI and reporting of the results
- Analysis of the results, including thermo-hydraulic, electro-magnetic, and structural simulations of the real operating conditions of the coil
- Analysis of impact of results on ITER PF coils design

#### 2006 ACTIVITIES

For 2006, activities were reduced because of the delay taken in the fabrication of the PFCI at Tesla (UK). However, some significant work was performed to prepare the PFCI tests by predicting conductor DC performance, conductor AC losses, and intermediate joint AC losses. The results of these predictive analyses have been presented together with analyses from other laboratories at the 2006 Applied Superconductivity Conference in Seattle (USA), August 29-September 1, 2006 [1].

#### PREDICTION OF CONDUCTOR DC PERFORMANCE

Predictive simulations have been performed on the basis of the PFCI test program. The main features of the model used for calculations are as follows:

- 3D geometrical computation for strands trajectories considered for 240 individual strands equivalent to one main subcable (petal), with a longitudinal increment of 10 mm.
- Strand/field angle effect is considered along the trajectories, with an anisotropy factor  $P = 0.3$
- A constant longitudinal temperature gradient along the conductor was assumed
- Strand temperature is assumed equal to helium temperature
- The local magnetic field on strands is obtained thanks to a 2D interpolation from the given computed data table provided by the Efremov Institute
- Uniform current density among strands inside the petal is assumed
- The strand transition  $n$  index is taken at  $n = 25$

Two current sharing temperature ( $T_{CS}$ ) tests have been chosen, with:  $I_{PFCI} = 18$  kA and  $I_{PFCI} = 45$  kA, respectively. For both tests, the applied magnetic field is  $B \sim 6$  T ( $I_{CSMC} \sim 21$  kA), the helium inlet temperature is  $T_{in}(t=0) = 4.5$  K, the helium inlet pressure is  $p_{in}(t=0) = 0.6$  MPa, the helium mass flow rate is  $dm/dt(t=0) = 10$  g/s and the temperature increase rate is  $dT/dt = 1$  mK/s.

The overall results are shown in figures. 1 a) and b) for 18 kA and 45 kA, respectively. Comparisons are made with the models developed by different institutes: NM for LLNL Livermore (USA), THELMA for Politecnico Torino (Italy), RW for CRPP Villigen (Switzerland), LZ for CEA (France) and EZ for Efremov Institute (Russia).

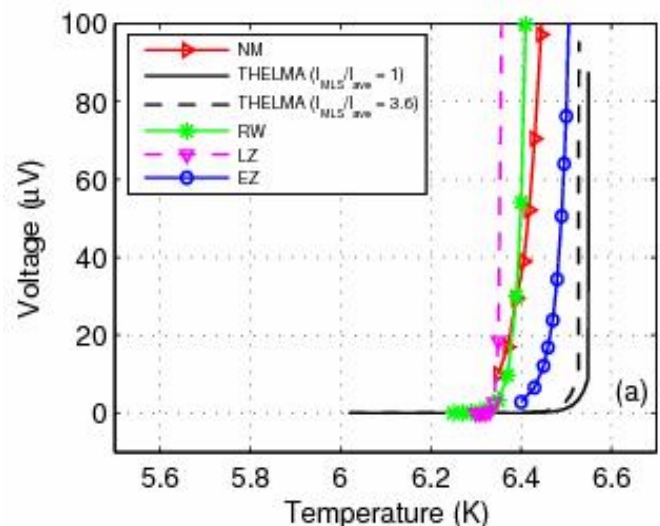


Figure 1a): Total voltage drop across PFCI coil main winding vs. helium inlet temperature at 18 kA.

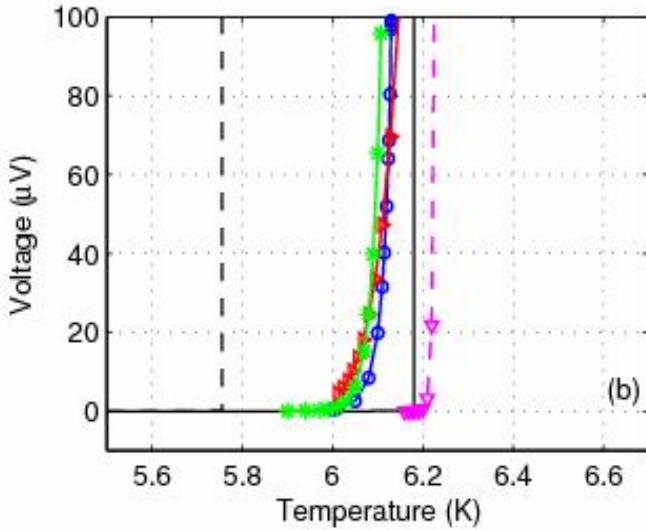


Figure 1b): Total voltage drop across PFCI coil main winding vs. helium inlet temperature at 45 kA

As can be seen, some differences appear between predictions which can be commented as:

- At  $I_{PFCI} = 18$  kA, a smooth transition is computed by several predictors, (see figure 1a) with  $T_{CS}$  in the range 6.35-6.55 K. The practically sudden transitions predicted by LZ and (to some extent) THELMA, with run away before a measurable voltage is reached, could be due both to the large  $n$  value assumed (LZ) and/or to overestimation of local effects (THELMA) already noted in the PFIS sample analysis.
- At  $I_{PFCI} = 45$  kA, the nature of the predicted transition depends even more on the model used. A sudden quench is predicted by THELMA and LZ, but the quench temperature strongly depends on the assumption of the current overload in the most loaded strands (MLS) in THELMA

### CONDUCTOR AC LOSSES CALCULATION

Simulations have been performed with the THEA code in order to calculate AC losses and thermal-hydraulic behaviour of the conductor winding, i.e. replacing lower terminal and intermediate joints by conductor, under CSMC exponential discharge and trapezoidal runs. Calculations have thus been performed considering a 44.2 m long conductor.

The AC losses calculation has been introduced in THEA and is based on classical formula for hysteretic and coupling losses in a cable. The main data characterizing the cable are:

- A time constant  $n\tau$  taken equal to 20 ms (at the cable scale, corresponding to  $N \sim 100$  cycles) [2],
- A NbTi filament effective diameter  $d_{eff} = 5 \mu m$ ,
- The scaling law parameters describing the critical current density  $J_c(B,T)$  in NbTi [3].

For the thermal-hydraulic behaviour, the correlations taken into account are:

- $f_{central} = 4,37 \cdot 10^{-2}$
- and  $f_{annular} = 1 / (\text{void}^{0,742} \cdot (0,0231 + 19,5/Re^{0,7953}))$  for friction factors,
- The Colburn-Reynolds analogy for heat exchange coefficients [4].

The first calculation deals with an exponential discharge of the CSMC with no current in the PFCI :  $I_{CSMC}(t=0) = 21,2$  kA, time constant = 20 s. The second calculation considers a CSMC trapezoidal wave of the CSMC current with again no current in the PFCI :  $I_{CSMC} = 21,2$  kA at flat top,  $dB/dt = \pm 5$  T/s, flat top duration = 5 s. For both simulations, the hydraulic conditions are  $T_{in} = 4,5$  K,  $P_{in} = 6.10^5$  Pa,  $dm/dt = 10$  g/s. Figure 2 shows predicted evolutions of the Joule power deposited in the conductor for both scenarios.

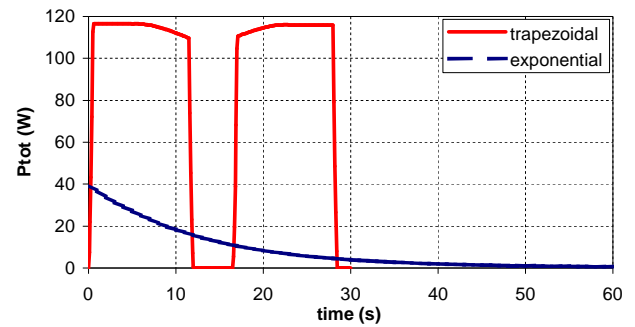


Figure 2: Evolution of the power deposited in the PFCI conductor

For the exponential mode, the maximum heat power is of  $\sim 40$  W at the beginning of the discharge. The total energy deposition reaches 525 J and the final temperature increase at the conductor outlet should be weak, near 0.05 K. In the trapezoidal scenario, the heat power induced reaches nearly 120 W during ramp up and ramp down, leading to an energy deposition of 2611 J. The outlet temperature increase is thus more important, about 0.25 K.

### INTERMEDIATE JOINT AC LOSSES CALCULATION

AC losses in the intermediate joint were computed using the JUST code developed by CEA [5]. Whereas in [3] the simulation was performed for the exponential decay of the CSMC current, the new simulation dealt with the trapezoidal run (see above). The code can separate the losses coming from the variation of the radial component of the field ( $W_r$ ) from the losses coming from the variation of the axial component of the field ( $W_z$ ), which is valid as long as no saturation of strand currents occurs.  $W_r$  comes mainly from induced currents crossing the joint mid-plane, these currents involve a large time constant ( $> 5$  s) inversely proportional to the joint DC resistance (here a realistic value of 5.1 nΩ has been taken).  $W_z$  comes mainly from eddy currents in copper pieces and interstrand coupling currents in the cables, these currents are characterized by low time constants ( $< 0.5$  s) which are independent of the joint DC resistance.

Figure 3 shows the results of the calculation:  $W_r$ ,  $W_z$ , and  $W_{tot} = W_r + W_z$  (total loss power), as functions of time during the trapezoidal run. The high value of  $W_z$  comes from the highest value of  $dB_z/dt$  compared to  $dB_r/dt$ , where  $B_r$  and  $B_z$  are the radial and axial magnetic field components, respectively. Compared to figure 2, one can see that the intermediate joint itself will provide roughly the same loss power as the whole regular winding of the coil.

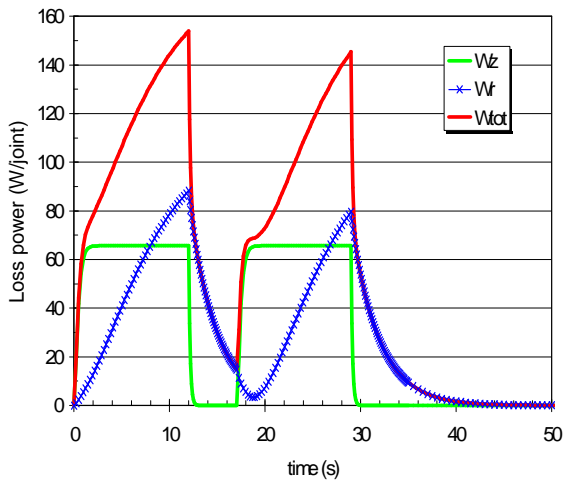


Figure 3: Loss power in PFCI intermediate joint during the CSMC current trapezoidal wave

## CONCLUSIONS

The fabrication of the Poloidal Field Conductor Insert (PFCI) has been completed in industry and the coil should be tested in the CSMC facility (Naka, Japan) in 2008. Within EFDA task PFCITE, we have adapted and used our codes to predict the conductor DC performance (current sharing temperature runs), as well as the AC losses in the regular conductor and in the intermediate joint. Due to the peculiar structure and geometry of the joint, the AC losses of the joint are expected to be at the same level as the AC losses in the whole regular conductor winding.

## REFERENCES

- [1] R. Zanino et al., "Predictive Analysis of the ITER Poloidal Field Conductor Insert (PFCI) Test Program", presented at the 2006 Applied Superconductivity Conference, Seattle (USA), Aug. 29-Sep. 1, 2006.
- [2] Yu. A. Ilyin, et al., "Effect of cyclic loading and conductor layout on contact resistance of full-size ITER PFCI conductors," IEEE Trans. Appl. Supercond., vol. 15, pp. 1359 – 1362, 2005.
- [3] R. Zanino, et al., "Preparation of the ITER Poloidal Field Conductor Insert (PFCI) Test," IEEE Trans. Appl. Supercond., vol. 15, pp. 1346 – 1350, 2005.

- [4] S. Nicollet et al, "Evaluation of the ITER Cable-In-Conduit-Conductor heat transfer" ICEC 20 (2004) 589 – 592.

## REPORTS AND PUBLICATIONS

- [5] D. Ciazynski and A. Martinez, "Electrical and thermal designs and analyses of joints for the ITER PF coils," IEEE Trans. Appl. Supercond., vol. 12, pp. 538–542, 2002

## TASK LEADER

Daniel CIAZYNSKI

DSM/DRFC/STEP  
CEA-Cadarache  
F-13108 Saint-Paul-Lez-Durance Cedex

Tel : 33.4.42.25.42.18

Fax : 33.4.42.25.26.61

e-mail : daniel.ciazynski@cea.fr

## TW5-TMSF-HTSMAG

### Task Title: SCOPING STUDY FOR HTS FUSION MAGNETS

#### INTRODUCTION

Will the superconducting system of DEMO [1] be simply an extrapolation of the superconducting system of ITER, or is it necessary to prepare for a complete technology mutation ?

This has to be considered as a function of the objectives of DEMO which are up to now not completely defined. This mutation could deal with the superconducting material if classical A15 superconducting materials cannot sustain the magnetic field of DEMO. But, even if A15 materials are still on the stage, it is not sure that the major components or choices of ITER should be adequate for DEMO as well: plates, conductor shape, mode of cooling etc

#### 2006 ACTIVITIES

##### A COMPARISON BETWEEN BI2212 AND Nb<sub>3</sub>Sn FOR THE TF MAGNET SYSTEM OF A DEMO TYPE REACTOR

For a tokamak, it will be admitted that, in a first approach, a performance factor  $\xi$  can be defined. If  $\xi$  is constant the fusion power and the amplification factor of the reactor are constant:  $\xi = R^2 B_t^3$ .

Regarding the general dimensioning of the tokamak, it has been shown in [1] and [2], that the maximum field on the magnet system situated at  $r_e$  (see figure 1), plays a very important role. In addition the leading role of the structure to resist the mechanical load, has been also demonstrated, highlighting the importance of the “radial built” of the machine ( $r'_i - r_o$ ). The overall current density if the TF system  $J_{cond}$  is driven by the structure.

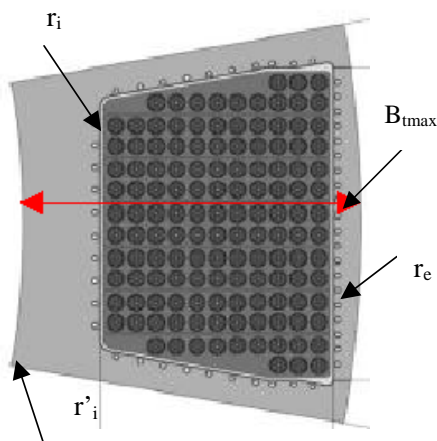


Figure 1: ITER inner leg showing the relative importance of structural components (plates and casing) and localization of maximum magnetic field

The discussion will be illustrated through the design of three fusion machines: ITER, DEMO1 and DEMO2 (see table 1).

A priori, high toroidal magnetic fields should be beneficial, because leading to smaller machines associated with lower investment cost.

Table 1: TF radial extension of ITER and of two versions of DEMO

	ITER	DEMO1	DEMO2
R (m)	6.2	7.5	8.5
a (m)	2.	2.5	2.83
$\xi$ (m <sup>2</sup> T <sup>3</sup> )	5723	12150	12150
B <sub>t</sub> (T)	5.3	6.	5.5
B <sub>tave</sub> (T)	11.02	13.62	11.78
B <sub>tmax</sub> (T)	11.8	14.6	12.6
B <sub>effective</sub> (T)	11.2	14.1	12.2
r <sub>e</sub> (m)	3.075	3.4	4.067
r <sub>i</sub> (m)	2.5	2.25	3.4
r' <sub>i</sub> (m)	2.17	1.76	2.945
J <sub>cond</sub> (A/mm <sup>2</sup> )	12.2	9	10.1

DEMO1 is the presently considered version of DEMO, with a major radius of 7.5 m; DEMO2 is an alternative version with a higher major radius (8.5 m) and, for the same  $\xi$ , associated with a lower toroidal magnetic field. As visible in table 1, the impact is important especially for  $r'_i$  which are different by 1.2 m for the two machines. It can be noted that the initial difference in major radius, which was 1 meter, has been amplified at the level of the inner radius of the radial extension to 1.2 m due to the high magnetic load of DEMO1.

Moreover this preliminary estimation shows that DEMO1 is probably, at given  $\xi$ , the machine with the smallest radius possible, taking into account the mechanical constraints

##### Discussion about the superconducting material of DEMO1 and DEMO2 TF system

The estimated capability of the actual industrial superconducting strands, developed in the framework of fusion programs, is presented in figure 2. The indicated temperature is not the operation temperature, but is the temperature including the margin, which drives the superconducting section when dimensioning the conductor.

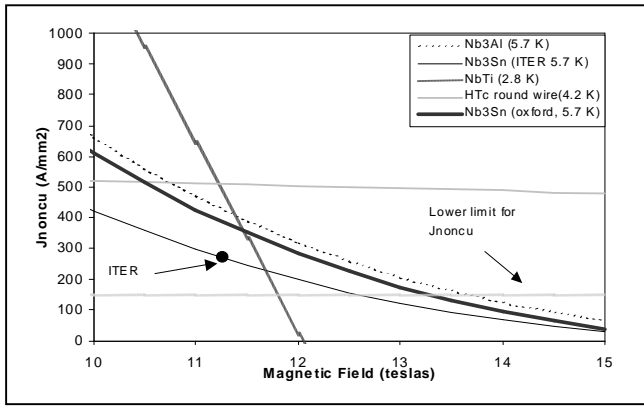


Figure 2: Capability of several industrial strands at different design temperatures

If a solution with actual low Tc industrial strands, exists for DEMO2 ( $B_{\text{effective}}=12.2$  T), according to figure 2, no industrial low Tc strand is available at present for DEMO1 ( $B_{\text{effective}}=14.1$  T). For the present study, an arbitrary value of 150 A/mm<sup>2</sup> has been taken into account for both versions.

A very preliminary estimation of the investment cost of the two DEMO versions has been performed. The basis for this estimation is described in [3] and has been checked on ITER. The dimensioning parameters are given according to the different components.

The difference of cost between the two machines is low: about 1310 M€

Estimation of the electrical power for cryogenic refrigeration in DEMO1 and DEMO2

The basis of the extrapolation of electrical power for cryogenic refrigeration from ITER to DEMO has been presented in [4]. It is admitted that DEMO will be a steady state machine contrary to ITER. At 4.5 K and 80 K, the steady state losses are proportional to Ra. Pr1 and Pr2, the estimated electrical powers awaited respectively at 4.5 K and 80 K, are given in table 2. Note that, in both DEMO versions, the level of electrical power is acceptable with respect to the electrical power of the reactor, which is about 1000 MW.

Table 2: Estimation of electrical power associated with cryogenic refrigeration for DEMO1 and DEMO2

	DEMO1	DEMO2
Ra	18.75 m <sup>2</sup>	24.06 m <sup>2</sup>
Pr1 (4.5K)	7.8 MW	9.7 MW
Pr2 (80 K)	10.6 MW	13.6 MW

### WHICH TEMPERATURE FOR THE MAGNET SYSTEM OF DEMO

Using HTS materials it can be envisaged to increase the operation temperature of the TF system. Starting from the estimated losses at 5 K  $P_{5K}$ , it is possible to derive Pr1 using the following formula:

$$Pr1 = P_{5K} f \eta$$

$\eta$  being the Carnot efficiency,  $T_2$  the magnet temperature and  $T_1$  the room temperature.

$$\eta = T_2 / (T_1 - T_2) \quad f \approx 0.25$$

Adjusting Pr1 arbitrarily at 10 MW (see table 2) for the magnet operation at 4 K, it is possible to see in figure 3 the impact of the coil operating temperature increase on Pr1.

This rough calculation supposes in a first approach, that the power to be extracted is not dependent on the operating temperature. It is visible in figure 3 that there is little interest to increase the temperature above 20 K.

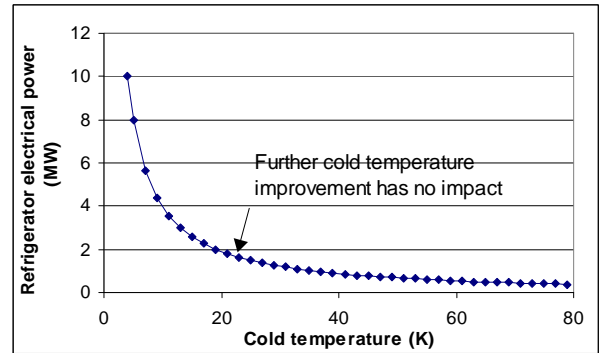


Figure 3: Impact of the coil temperature on the refrigerator electrical power Pr1

However using a circulation loop at 20 K and a cryoplant at 4.2 K is very costly due to the low density of helium at 20 K and therefore the high dissipated power in the pump to compensate pressure drop in magnets. Indeed, this scheme is more efficient if fully operated at 4.5K, therefore the operation of HTS magnets at 4.5 K should be also envisaged as it would also provide significant operation margins, to the magnets. It is also suggested not to use hydrogen cycle as it does not bring many benefits in terms of electrical consumption, and also considering the risks and safety issues added to the system.

From the cryoplant point of view, operating magnets at 20 K instead of 4 K will have a significant impact on reduction of electrical consumption. However, the flexibility will not be the same due to the lack of temperature reference and buffering that can provide a liquid bath

### CONCLUSIONS

Considering the high level of recirculating power presently envisaged for DEMO which is 544MW, the electrical power estimated for the magnet system of DEMO and derived from ITER which is around 20 MW is not a major concern.

Therefore the conclusion of this study is that there is no absolute need to envisage a technical revolution for the magnet systems of DEMO in designing a magnet system operating at higher temperature than 5 K.

However the design of DEMO is not completely finalized and therefore an R&D program is to be maintained in the direction of HTS, it appears from this report that there is no interest in terms of efficiency to operate the magnet system

above 20 K, the largest expected reduction of electrical energy consumption being already reached at this level.

With respect to this consideration, Bi2212 conductors have made during the last five years, a lot of progress, with the production of long unit length, round strands, and prototype cables. **They therefore appear as the best candidates from far.**

In the present design of DEMO, it appears that the maximum magnetic field on the conductor will be in the range of 12 to 14 T. This range of magnetic field could probably be within reach of conventional A15 materials like Nb<sub>3</sub>Sn if the present problems regarding strain sensitivity due to Lorentz forces are mastered which looks probable.

If not, again Bi2212 due to their industrial maturity are well placed and should be developed.

## TASK LEADER

---

Jean-Luc DUCHATEAU

DSM/DRFC/STEP

CEA-Cadarache

F-13108 Saint-Paul-Lez-Durance Cedex

Tel. : 33 4 42 25 49 67

Fax : 33 4 42 25 26 61

e-mail : jean-luc.duchateau@cea.fr

## REPORTS AND PUBLICATIONS

---

- [1] J.L Duchateau, P. Hertout, J. Johner "Discussion about the Size of a Future Fusion Demonstration Reactor: the Impact of the Toroidal Magnetic Field" Invited paper at Applied Superconductivity Conference. Seattle (USA) September 2006. To be published
- [2] J.L Duchateau, J.M. Rey, P. Roussel. February 2007 "task HTSMAG-TW5-TMS-HTSMAG final report" Internal report AIM/NTT-2007.004
- [3] P. Hertout, "Algorithm for cost evaluation of tokamaks with copper or superconducting magnets," (2004) Internal note AIM/NTT-2004.002
- [4] J.L Duchateau, J.Y. Journeaux, F. Millet, "Estimation of recycled power associated with cryogenic refrigeration power of a fusion reactor based on TORE SUPRA experiment and ITER design," Nucl. Fusion 46 (2006) 94-99

## TW5-TMSF-HTSPER

### Task Title: HTS MATERIALS FOR FUSION MAGNETS

#### INTRODUCTION

High Tc superconductors are just coming out of the R&D stage. Long term work will be needed until the availability of such conductor for fusion plant. Among the potential superconducting HTS materials Bi(2,2,1,2) seems the most advanced in term of industrial production as well as suitability for large superconducting magnets. Furthermore it is the only superconducting material allowing the drawing of round wire usable for cabling with conventional cabling machines.

This high Tc superconducting material will be studied in order to identify its engineering performance and the parameters limiting its use. Emphasis will be given in electrical properties with the aim to provide data for the TW5-TMSF-HTSMAG task.

Following the manufacturing of a cryostat insert allowing the critical current to be measured up to 40K the experimental measurements have started.

#### 2006 ACTIVITIES

##### STATE OF THE ART IN Bi2212 SUPERCONDUCTOR PRODUCTION

The Nexans Company has been working since several years on a 800 kJ SMES (Superconducting Magnetic Energy Storage) operating at 20 K and with a local maximum field of 7 T. This SMES has been successfully tested in 2006. The conductor produced by Nexans in length up to 1000 m contains 85 superconducting filaments in a silver matrix. The outer shell of this matrix is made of AgMg alloy as a strengthening element. The section of this conductor is 4 x 0.25 mm<sup>2</sup>. Its current transport property reaches up to 500 A/mm<sup>2</sup> at 4.2 K and 20 T at the maximum but the mean value is between 100 and 150 A/mm<sup>2</sup> at 4.2 K and 20 T. This is the conductor tested in our test station between 4.2 K and 40 K.

In a complementary activity initiated by CEA-Saclay a round wire has been developed at Nexans and produced during 2006. A picture of this new wire is shown on figure1.

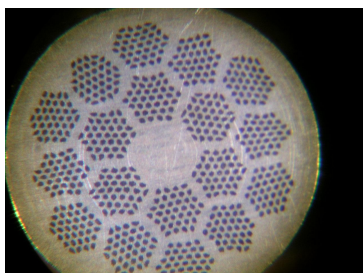


Figure 1: Cross section of a Bi(2,2,1,2) round wire developed by Nexans under CEA contract.

Diameter 0.8 mm

#### TEST STATION UPGRADE

The CétaCÉS test station is dedicated to critical current measurement under high field. Samples of superconducting wires can be tested up to 3000 A at 4.2 K in a magnetic field up to 16 T. A thermal regulation allowing measurements between 1.8 and 4.2 K has already been developed. Tested samples are usually Nb<sub>3</sub>Sn wires used in VAMAS samples.

A new sample holder has been developed allowing critical current measurement in the 5 K to 40 K range. This special insert is based on a helium gas thermal regulation. Special attention has been paid to limit the thermal gradient in the sample area. Figure 2 is a picture of the upgraded facility showing the phase separator used to eliminate the liquid helium and adjust roughly the temperature of the gaseous helium and the test station itself.

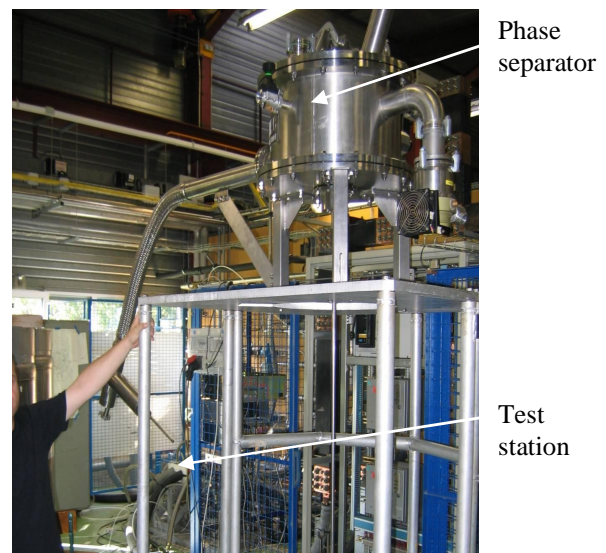


Figure 2: The upgraded CETACES test facility

To limit the thermal losses in the sample area the 500 A current feed trough are made of superconducting ribbons of the type produced by Nexans.

The new facility has been assembled and tested during thesecond half of 2006 and worked satisfactorily.

#### TEST SAMPLE DEVELOPMENT

In parallel to the development of the test station, new types of samples have been designed. A VAMAS like sample holder will be used to measure the critical current of the HTc ribbons. In order to study the influence of residual stresses in the superconducting material these VAMAS like sample holder will be realised in different materials: titanium alloy, aluminium alloy, copper, stainless steel and glass fiber epoxy composite.

A wind and react way to test the sample has been developed using an Inconel mandrel to react the superconducting ribbon which is afterwards transferred on the measurement VAMAS mandrel. Figure 3 shows a VAMAS sample after the transfer.



Figure 3: HTs ribbon on a VAMAS mandrel

**MEASUREMENT OF CRITICAL CURRENT AND CRITICAL CURRENT DENSITY UP TO 40K**

Measurements are going on at CEA-Saclay and some preliminary results are available. As shown on figure 4 the noise level on the superconducting part of the V/I plot is not a function of temperature. The criterion used for HTs material is the same as the one used for conventional low temperature superconductors, 1.0 microV/cm.

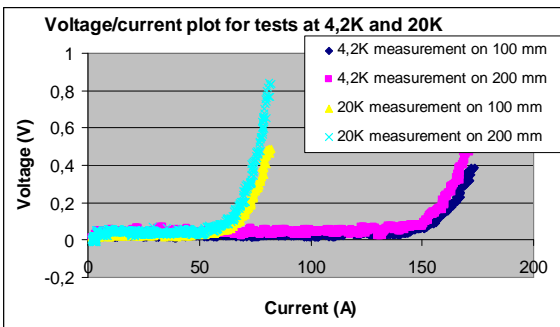


Figure 4

**CRITICAL CURRENT AS A FUNCTION OF MAGNETIC FIELD**

As expected the critical current reduces with magnetic field. Figure 5 shows the reduction in critical current between 7 and 15 T.

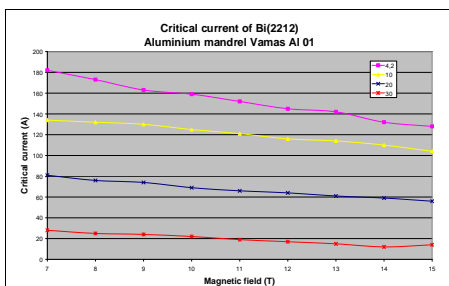


Figure 5

**CRITICAL CURRENT AS A FUNCTION OF TEMPERATURE**

The extrapolation of previous curves allows estimating the critical field as a function of temperature which is shown on figure 6. The very surprising result is not explained actually.

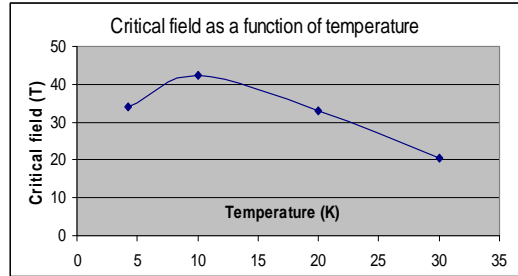


Figure 6

**COMPARISON BETWEEN DIFFERENT RIBBONS SUPPOSEDLY IDENTICAL**

There is a wide scatter in the results obtained for ribbons supposed identical and tested in the same condition. Figure 7 provides the critical current results of 2 ribbons tested on aluminium alloy mandrels. Such differences are supposed to come from slight deviation in the composition of the powder mixture.

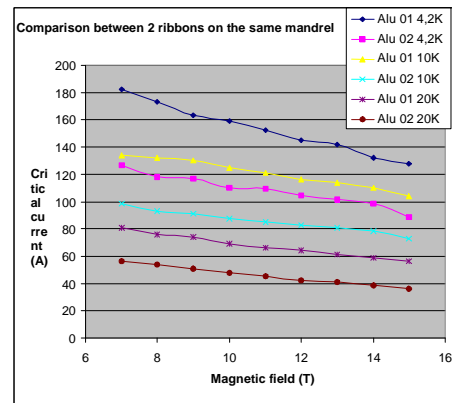


Figure 7

**CRITICAL CURRENT AS A FUNCTION OF RESIDUAL STRESSES**

The use of different materials for the VAMAS mandrels allows plotting the result as a function of the mandrel thermal contraction as shown on figure 8. Further work is needed to define precisely the residual strain of the tested samples.

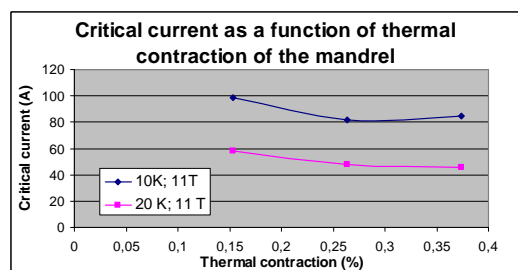


Figure 8

## **CONCLUSIONS**

---

Although some delays have been encountered with the upgrading of the CETACES test station, the work is progressing well and the characterization of the HTs materials has started.

In order to have significant error bars the systematic duplication of the measurements is needed to estimate the respective contributions of heat treatment, powder mixture in the superconductor precursors and assembling on the test station.

## **TASK LEADER**

---

Jean-Michel REY

DSM/DAPNIA/SACM/LEAS  
CEA-Saclay  
F-91191 Gif-sur-Yvette-Cedex

Tel. : 33 1 69 08 66 85

Fax : 33 1 69 08 69 29

e-mail : [jmrey@dapnia.cea.fr](mailto:jmrey@dapnia.cea.fr)

**TW6-TMSC-FSTEST****Task Title: PARTICIPATION TO CONDUCTOR TESTS AND EVALUATION OF TEST RESULTS****INTRODUCTION**

In the framework of the EFDA Technology Work programme, additional full size conductor samples are being manufactured and tested in order to assess the gain in performance by using advanced Nb<sub>3</sub>Sn strand. The scope of this work can be summarised as follows:

- Preparation of the test programme and review of the instrumentation;
- Predictive DC performance analyses and the basis of the strand data;
- Participation in the testing campaigns for TF/PF conductors;
- Evaluation of the test results;
- Preparation of the Final Report describing the main results and conclusions extrapolated from the testing campaigns.

Two samples (TFAS1 and TFAS2) based on the Toroidal Field Model Coil (TFMC) conductor design were tested in 2005-2006, two other samples (TFPRO1 and TFPRO2) based on the ITER TF conductor design should be tested in the first half of 2007, and a fifth sample (NEFSS) using an ITER TF-type conductor fabricated by the Russian Federation should be tested in July 2007. Only four samples were considered initially in the task.

**2006 ACTIVITIES**

CEA Euratom-Association participated in the extensive test of TFAS1, conducted the preparation of the TFAS2 testing program [1] and participated in the test of TFAS2. The tests were performed in the SULTAN facility at CRPP Villigen (Switzerland). Our Association also contributed to the reduction of the experimental data [2], and to the analysis of the test results with regard to the properties of the strand composing the tested conductors, as well as with regard to the expected performance for the ITER TF conductor [3]. Our Association presented the test results at the 24<sup>th</sup> SOFT Conference held in Warsaw (Poland) on September 11-15, 2006 [4] and contributed to presentations of the test results at the 2006 Applied Superconductivity Conference, held in Seattle (USA) on August 29-September 1, 2006 [5],[6].

**SHORT DESCRIPTION OF TFAS1 and TFAS2**

TFAS1 and TFAS2, as all the big SULTAN samples, are composed of two straight conductor legs connected together at one end through an electrical joint and having each at the other end a terminal joint to connect the sample to the facility transformer. The four conductor legs are based on the TFMC conductor design (see figure 1) but each of them makes use of a different advanced superconducting (s/c) strand produced by an European company:

European Advanced Superconductors (EAS) using the bronze route, Oxford Instruments (OST), Luvata Pori (OKSC) and Luvata Italy (OCSI) using internal tin. Only the number of s/c strands and the number of pure copper (Cu) strands are varied to match strand current capability (see table 1). The TFMC conductor itself had 1/3 of Cu strands. The samples are about 3.5 m long (including the joints), but only a conductor length of 450 mm (about one cable twist pitch) can be submitted to a high magnetic field in the facility.

*Table 1: Strands in TFAS1 and TFAS2 conductors*

Leg	Strand	S/c strands	Cu strands
TFAS1-Right	OST	720	360
TFAS1-Left	EAS	1080	0
TFAS2-Right	OKSC	720	360
TFAS2-Left	OCSI	1080	0

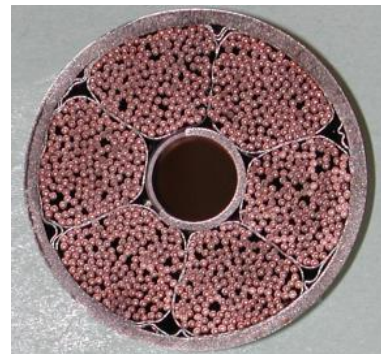


*Figure 1: Cross-section of TFAS2 OCSI conductor*

**TEST RESULTS AND ANALYSIS FOR TFAS1**

A first testing campaign was carried out under different magnetic fields from 11 T down to 8 T by 1 T steps. Then 1000 current cycles from 0 to 60 kA and back to 0, under a 11 T field, were applied to perform a mechanical cycling under the Lorentz force. After cycling, the sample was again tested in a second campaign, similarly as in the first campaign. Since it was observed that the temperature sensors mounted on the sample were not accurate enough, likely due to an insufficient thermalisation, a third testing campaign was performed after installation by CRPP of additional temperature sensors. This third campaign was thus used to confirm conductor performance as well as to calibrate the “old” sensors in order to be able to use the results of the first two campaigns.

A first unexpected experimental result was the observation of an “extra” voltage drop on all the measured voltage drops used to define the electrical field developed along the conductor, and therefore used to define the conductor performance.

This disturbing effect, which could be observed even at zero applied magnetic field and low temperature (4.5 K), could be either positive or negative depending on the conductor and on the voltage taps, and was varying roughly linearly with the sample current. In addition, this effect was found to vary slightly with applied magnetic field and with sample history. As this extra voltage drop could be at high current (70 kA) as high as the electric field criterion (10  $\mu\text{V/m}$ ) used to define the conductor current sharing temperature ( $T_{cs}$ ), it was decided to remove (compensate) it on the experimental voltage drop used to define conductor performance. The origin of this effect was thought to come from slightly different electric potentials among the conductor main subcables due to non-perfect electrical joints. The original idea was to compute the compensation by using runs performed at zero magnetic field and 4.5 K for which a real resistive behaviour of the superconducting conductor could not be suspected [2].

A second remarkable experimental result was the degradation of the conductor performance (particularly of the OST leg) from run to run (including cycling) which made the last test (3<sup>rd</sup> campaign)  $T_{cs}$  to be about 0.4-0.5 K lower than the very first values on the EAS leg, and about 1 K lower on the OST leg (see figures 2 and 3).

The ITER-type  $\text{Nb}_3\text{Sn}$  conductor performances are generally assessed with respect to strand performance using smeared models. A fully reversible degradation can be modeled by adding an extra strain  $\epsilon_{\text{extra}}$  (proportional to the total Lorentz force on the conductor) to the thermal strain  $\epsilon_{\text{th}}$  of the  $\text{Nb}_3\text{Sn}$  filaments, whereas a fully irreversible degradation of the strand current capability can be modeled by applying a coefficient  $\alpha_{\text{eff}} (< 1)$  to the conductor critical current computed (from strand properties) with only the thermal strain.

Figures 2 and 3 show the experimental points obtained during the three campaigns, on the OST and the EAS legs, respectively, together with a fit of the points of the 3<sup>rd</sup> campaign obtained using the irreversible smeared model. The associated values of  $\epsilon_{\text{th}}$  and  $\alpha_{\text{eff}}$  giving the best fit at 11 T are reported in table 2. Note also that the fit is not so good at 8 T for the EAS conductor.

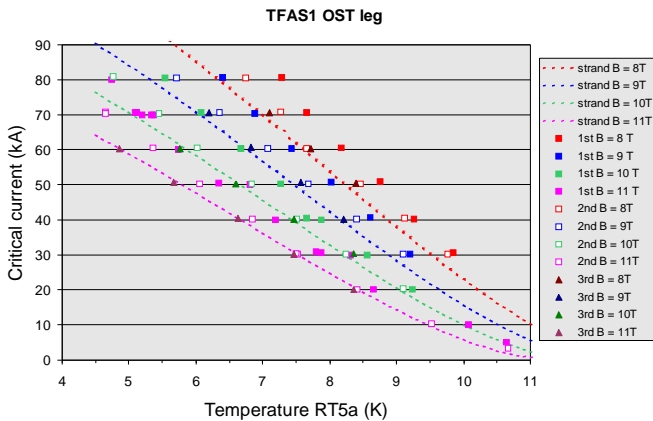


Figure 2: Test results (1<sup>st</sup>, 2<sup>nd</sup>, 3<sup>rd</sup> campaigns) and analysis from strand properties (best fitting 3<sup>rd</sup> campaign at 11 T) on TFAS1 OST conductor

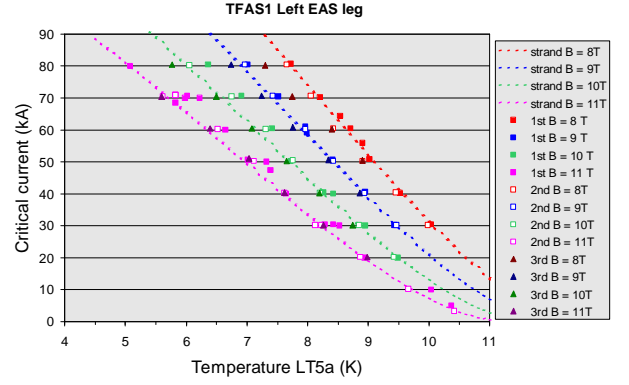


Figure 3: Test results (1<sup>st</sup>, 2<sup>nd</sup>, 3<sup>rd</sup> campaigns) and analysis from strand properties (best fitting 3<sup>rd</sup> campaign at 11 T) on TFAS1 EAS conductor

### TEST RESULTS AND ANALYSIS FOR TFAS2

Extra voltage drops were also observed on TFAS2, but this time special dedicated runs with 10 kA step by step increase of the sample current, under a given magnetic field, were applied in order to compute accurately the compensating voltage drops. Note that the use of clamped copper rings around the conductor jacket, to create a kind of equipotential surface averaging the subcables potentials, did not produce its expected beneficial effect on voltage drop. On the other hand, this time the temperature sensors were mounted properly and the temperature measurements were quite reliable. A first testing campaign, similar to TFAS1, was first carried out, then 1000 current cycles from 0 to 68 kA (ITER TF current) and back to 0, under a 11 T field were applied, and finally a second testing campaign similar to the first one was carried out to check the conductor “after cycling” performance. In addition, after warm-up and cool-down, a third campaign was dedicated to thermohydraulic tests with only a few (not accurate) electric tests.

Again, a degradation with “cycling” was observed, however with a lower extent than in TFAS1. Figures 4 and 5 show the experimental points obtained during the three campaigns, on the OKSC and the OCSI legs, respectively, together with a fit of the points of the 2<sup>nd</sup> campaign obtained using the irreversible smeared model. The associated values of  $\epsilon_{\text{th}}$  and  $\alpha_{\text{eff}}$  giving the best fit at 11 T are reported in table 2. Note also that the fit is not so good at 8 T for the OCSI conductor.

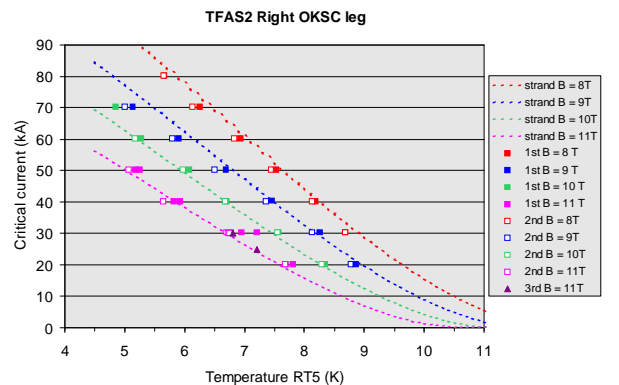


Figure 4: Test results (1<sup>st</sup>, 2<sup>nd</sup>, 3<sup>rd</sup> campaigns) and analysis from strand properties (best fitting 3<sup>rd</sup> campaign at 11 T) on TFAS2 OKSC conductor

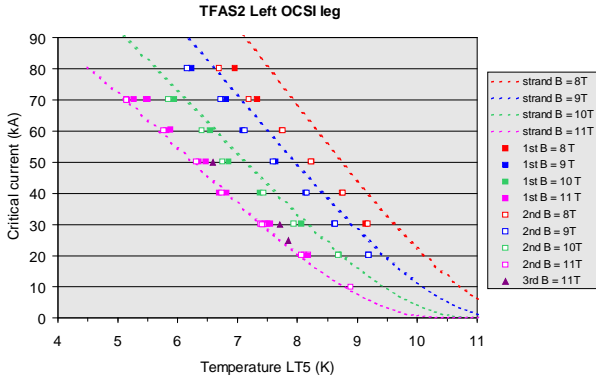


Figure 5: Test results (1<sup>st</sup>, 2<sup>nd</sup>, 3<sup>rd</sup> campaigns) and analysis from strand properties (best fitting 2<sup>nd</sup> campaign at 11 T) on TFAS2 OCSI conductor

Table 2: Best fit values of irreversible model parameters at B = 11 T after cycling

Conductor	$\epsilon_{th}$ (%)	$\alpha_{eff}$
TFAS1-OST	-0.36	0.41
TFAS1-EAS	-0.54	0.62
TFAS2-OKSC	-0.46	0.42
TFAS2-OCSI	-0.64	0.64

**EXTRAPOLATION TO ITER TF CONDUCTOR**

The most relevant operating conditions for the ITER TF conductors are those performed under an 11 T magnetic field. However, because all the TFAS conductors have different non-copper areas, to consider ITER TF relevant operating conditions means to consider operation at different currents, all different from the ITER TF conductor (68 kA). Table 3 gives the “equivalent” operating currents in the TFAS conductors as well as in the original TFMC conductor. Then the estimation of a TFAS conductor performance to the ITER TF conductor can only be made using extrapolations based on models. The two smeared models depicted above have been used for this purpose. Note also that a slight correction has to be made to account for the different self-field values. The results of these extrapolations using the “after cycling” experimental points are given in figure 6 as current sharing temperature vs. run number. The extrapolations obtained from the original TFMC sample tested in SULTAN are also plotted. In the legend, m1 means the reversible “ $\epsilon_{extra}$ ” model, and m2 means the irreversible “ $\alpha_{eff}$ ” model. It is worth noting that the TFAS1 conductors were tested with a maximum Lorentz force (900 kN/m, corresponding to 80 kA under 11 T) in excess of the ITER TF nominal value (760 kN/m) during the first campaign (first series at 11 T), while such an overload was applied only “after cycling” tests to the TFAS2 conductors without any damage.

Table 3: Equivalent currents in tested conductors to operate at ITER TF non-copper current density

Conductor	OST	EAS	OKSC	OCSI	TFMC	ITER TF
$I_{eq}$ (kA)	53	83	51	65	42	68

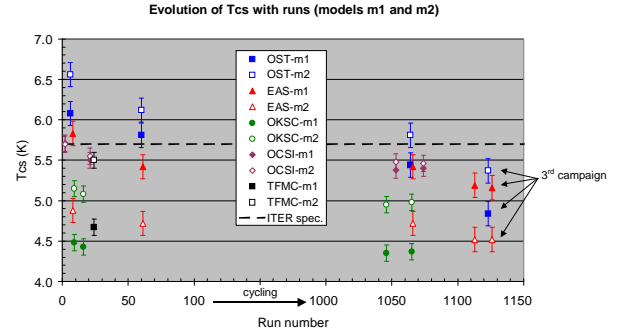


Figure 6: Evolution of TFAS and TFMC conductor  $T_{cs}$  with runs under ITER TF operating conditions

It can be seen in figure 6 that, whatever the model is, the extrapolated performance for any conductor after cycling and tests is always below the ITER TF specification of 5.7 K. Except the OCSI conductor, the other TFAS conductors do not appear much better than the original TFMC conductor. The scattering of the extrapolations depending on the model (except for OCSI) is also quite large, generally about 0.5 K or even higher.

**THERMOHYDRAULIC TESTS ON TFAS2**

Thermohydraulic tests were performed on TFAS2 to estimate the heat exchange coefficient H between the annular (strand) area and the central channel. The preliminary results obtained using steady state heating (measurement of the characteristic transfer length) are presented in table 4. It can be seen in this table that the CEA model predicts a correct order of magnitude as well as the correct evolution with the operating conditions (mass flow, temperature), however the model tends to underestimate by 30-40% the heat exchange.

Table 4: Comparison between H experimental and H given by the model

Testing conditions			H experimental (W.m <sup>-2</sup> .K <sup>-1</sup> )	H model (W.m <sup>-2</sup> .K <sup>-1</sup> )	H model / H experimental
T <sub>inlet</sub> (K)	Q (g/s)	W annular heater (W)			
4.61	5.73	8.59	536	379	0.71
5.98	5.09	5.47	665	455	0.68
6.55	4.63	6.30	780	471	0.60

## CONCLUSIONS

---

CEA-Euratom Association conducted the preparation of the testing programs and worked on predictive analyses for TFAS1 and TFAS2. Our Association participated in the three testing campaigns of TFAS1 and in the three testing campaigns of TFAS2 in SULTAN at Villigen (Switzerland), as well as in the analysis of the test results with regard to strand properties and with regard to the ITER TF conductor expected performance.

From the experimental point of view, both legs in both samples have been characterized by the observation of an extra voltage drop (either positive or negative) varying roughly linearly with the transport current but dependent on the applied magnetic field and the sample history. This voltage drop, never observed at this level on previous samples, has been attributed to current transfer among strands and petals. It has been corrected in the analysis of the V-I or V-T characteristics for each conductor because of the difficulty to consider it has a real resistive voltage (particularly when negative) and of the lack of experimental data to model it using an electrical network (as ENSIC at CEA).

With different behaviours, all these conductors show performance below the ITER TF  $T_{cs}$  specification, (the best conductor (OCSI) being about 0.3 K below the 5.7 K specification) and finally not much higher than the original TFMC conductor. These poor results have questioned the present ITER Nb<sub>3</sub>Sn conductor design.

The analysis of the results also shows that the present simple “smeared” models while useful to understand conductor performance from strand and to compare conductor behaviours, are not fully reliable to predict either conductor performance directly from strand properties or conductor performance in coils from performance in a short straight sample.

A dedicated test of TFAS2 also gave the opportunity to gather additional data on the heat transfer between annular channel and central spiral in the conductor, in order to validate existing thermal-hydraulic models.

## REPORTS AND PUBLICATIONS

---

- [1] D. Ciazynski, P. Bruzzone, L. Muzzi, B. Renard, L. Zani, “EFDA TASK TW6-TMSC-FSTEST: Testing Program for TFAS2 in SULTAN”, CEA Internal Note DRFC/STEP: AIM/NTT-2006.017, April 26, 2006
- [2] D. Ciazynski, “Problems with TFAS1 experimental data reduction (Voltage & Temperature)”, presented at the 2nd TFAS1 Testing Group Meeting, Frascati, March 30, 2005

- [3] D. Ciazynski with the collaboration of all the TG members from CEA, CRPP, ENEA, EPTO “Test Results and Analysis of TFAS1 & TFAS2”, presented at the ITER Conductor Meeting, Cadarache, July 24-25, 2006
- [4] D. Ciazynski, “Review of Nb<sub>3</sub>Sn Conductors for ITER”, presented at the 24<sup>th</sup> SOFT Conference (Warsaw, 11-15 Sep. 2006), accepted for publication in Fusion Eng. and Design
- [5] P. Bruzzone et al., “Test Results of two ITER TF Conductor short Samples using high Current Density Nb<sub>3</sub>Sn Strands”, presented at 2006 Applied Superconductivity Conference (Seattle, 29 Aug. – 1<sup>st</sup> Sep. 2006)., accepted for publication in IEEE Trans. on Appl. Supercond
- [6] L. Zani et al. “Analysis of DC Properties and Current Distribution in TFAS ITER Conductor Samples using high JC Nb<sub>3</sub>Sn advanced Strands”, presented at 2006 Applied Superconductivity Conference (Seattle, 29 Aug. – 1<sup>st</sup> Sep. 2006)., accepted for publication in IEEE Trans. on Appl. Supercond

## TASK LEADER

---

Daniel CIAZYNSKI

DSM/DRFC/STEP

CEA-Cadarache

F-13108 Saint-Paul-Lez-Durance Cedex

Tel. : 33 4 42 25 42 18

Fax : 33 4 42 25 26 61

e-mail : daniel.ciazynski@cea.fr